TABLE 1

Clinical Data Before and After Implantation of Artisan PIOLs in 60 Eyes of 36 Patients

Parameter	Preoperative	Postoperative	*P* Value*
Spherical equivalent refraction (D)	−12.40±2.30	−0.17±0.67	
UCVA (logMAR)	1.31±0.21	−0.051±0.17	
BSCVA (logMAR)	−0.11±0.072	−0.18±0.083	.0002
HOAs (μm)			
Total RMS	11.9±2.7	1.34±0.76	
Total HOA-RMS	0.21±0.16	0.33±0.26	.017
Coma-like aberration (S3)	0.14±0.16	0.27±0.17	.01
Spherical-like aberration (S4)	0.096±0.083	0.22±0.17	.01
AULCSF without glare	1.35±0.19	1.35±0.23	.886
AULCSF with glare	1.21±0.23	1.33±0.32	.018

Safety index: 1.18; efficacy index: 0.91
PIOL = phakic intraocular lens, UCVA = uncorrected visual acuity, BSCVA = best spectacle-corrected visual acuity, logMAR = logarithm of the minimum angle resolution, HOA = higher order aberrations, RMS = root-mean-square, AULCSF = area under the log contrast sensitivity function
**Paired t test.*

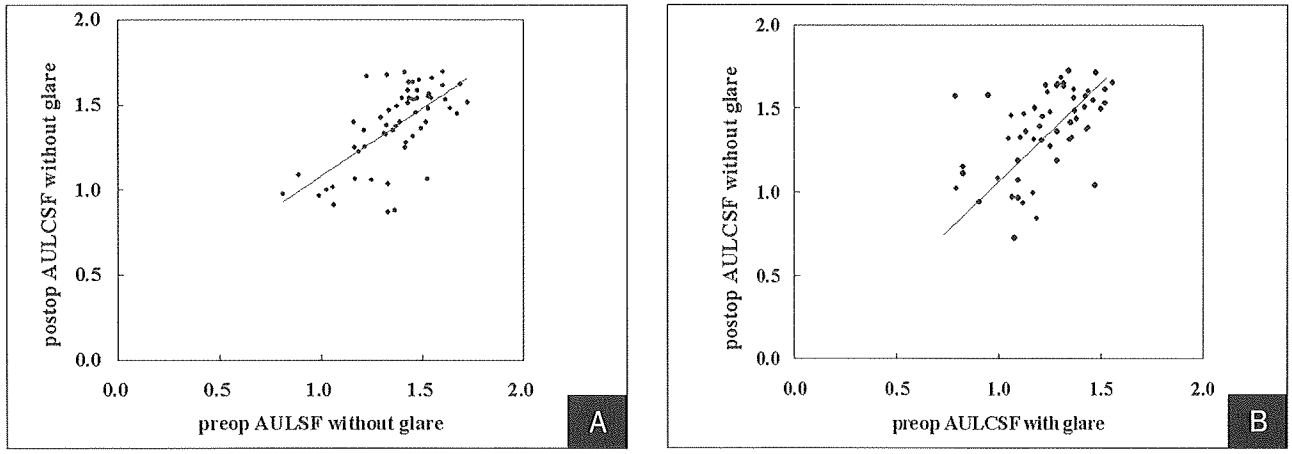

Figure 1. Correlation between the pre- and postoperative area under the log contrast sensitivity function (AULCSF) **A)** without glare and **B)** with glare (Pearson's correlation coefficient (a) r=0.77, *P*<.0001, (b) r=0.658, *P*<.0001).

The mean AULCSF with glare improved significantly postoperatively (*P*=.018). The postoperative AULCSF without glare was significantly correlated with the preoperative AULCSF without glare, and the postoperative AULCSF with glare was significantly correlated with the preoperative AULCSF with glare (Fig 1).

The results of stepwise regression analysis are shown in Table 2. The variables relevant to the postoperative AULCSF with or without glare were axial length and age. The preoperative refraction showed multicollinearity with the axial length. Postoperative S3 and S4 showed multicollinearity with age. Therefore, these parameters were not entered into the regression model. The multiple regression equations were as follows:

$$\text{Postoperative AULCSF (without glare)} = (-0.101 \times \text{axial length}) + (-0.008 \times \text{age}) + 4.56 \quad (R^2=0.261)$$

$$\text{Postoperative AULCSF (with glare)} = (-0.127 \times \text{axial length}) + (-0.012 \times \text{age}) + 5.31 \quad (R^2=0.368)$$

Standardized partial regression coefficients were assessed to discern the magnitude of the effect of each variable. The axial length was the most relevant variable followed by age (Table 2). The postoperative AULCSF was negatively correlated with axial length (Fig 2) and age (Fig 3). A positive correlation

TABLE 2

Results of Stepwise Regression Analysis to Select Variables Relevant to Postoperative Area Under the Log Contrast Sensitivity Function (AULCSF) With and Without Glare

Variables	Partial Regression Coefficient	Standardized Partial Regression Coefficient	*P* Value
AULCSF without glare			
Axial length (mm)	−0.101	0.579	.0002
Age (y)	−0.008	−0.227	.0063
Constant Adjusted R^2=0.261	4.56		
AULCSF with glare			
Axial length (mm)	−0.127	0.53	<.0001
Age (y)	−0.012	−0.237	.0294
Constant Adjusted R^2=0.368	5.31		

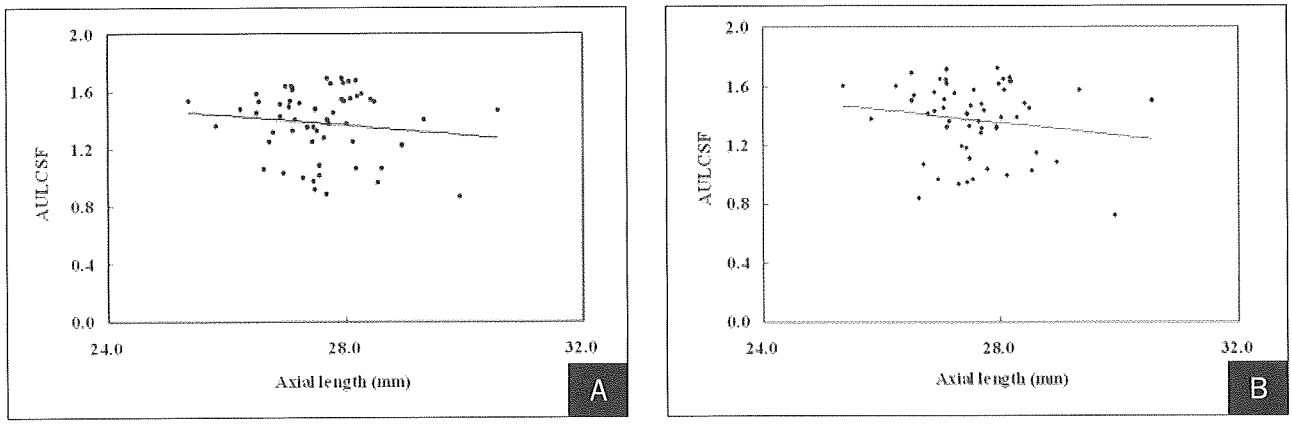

Figure 2. Correlation between the axial length and area under the log contrast sensitivity function (AULCSF) **A)** without glare and **B)** with glare (Pearson's correlation coefficient (a) r=−0.408, *P*=.0011, (b) r=−0.453, *P*=.0002).

was observed between postoperative S3 and age and between the postoperative S4 and age (Fig 4). The changes in S3 (ΔS3) and S4 (ΔS4) before and after surgery were correlated with age (Fig 5), but there was no significant correlation between the axial length and ΔS3 or between the axial length and ΔS4 (Fig 6).

DISCUSSION

Our results showed that patient age and axial length significantly affected the postoperative AULCSF, which is one of the indices of visual function, in eyes with Artisan PIOLs both with and without glare.

The results of multiple regression showed that the axial length was the most relevant variable, and it had a significant negative correlation with the postoperative AULCSF (see Fig 2). The preoperative refraction (the attempted correction) had a significant negative correlation with the axial length (*P*<.0001) and showed multicollinearity with the axial length.

Regarding the influence of axial length on visual function, Kora et al[24] reported visual acuity after cataract surgery in patients with high myopia decreases as the axial length increases. Visual function has also been reported to deteriorate in high myopia in normal eyes.[25,26] Jaworski et al[26] investigated the retinal integrity in high myopia using spatial psychophysical tasks and concluded that highly myopic eyes have either a reduced number of receptors, reduced sensitivity, or both, or reduced sensitivity of the postreceptoral processes. Those investigators also reported that the presence of normal contrast sensitivity at low spatial frequencies indicates dysfunction at a postreceptoral level in eyes with high myopia.[26]

In the current results, the axial length and preoperative refraction had a significant negative correlation with the postoperative AULCSF in eyes with Artisan

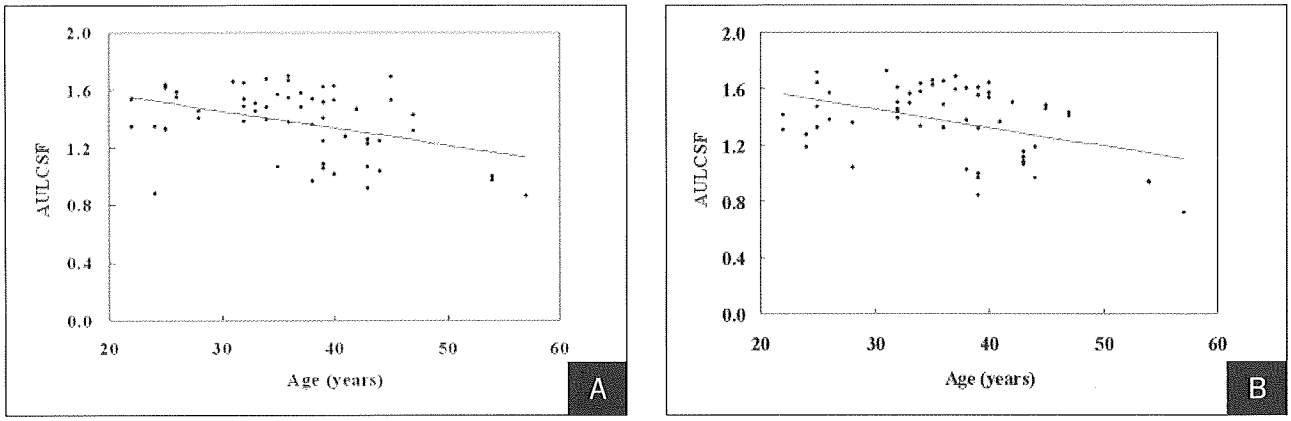

Figure 3. Correlation between age and the area under log contrast sensitivity function (AULCSF) **A)** without glare and **B)** with glare (Pearson's correlation coefficient (a) r=−0.466, *P*=.0057, (b) r=−0.492, *P*=.0031).

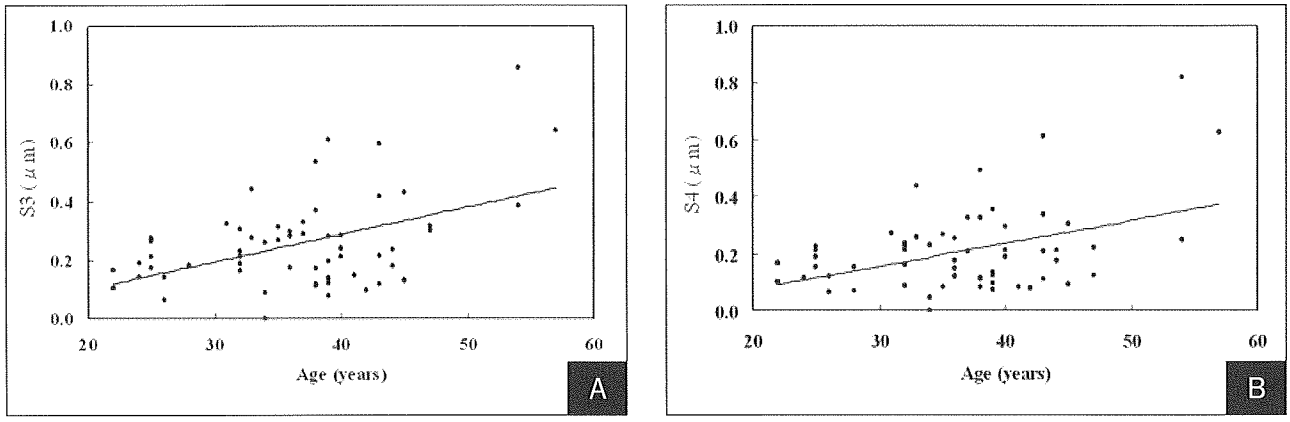

Figure 4. There is a significant correlation between age and **A)** S3 and **B)** S4 (Pearson's correlation coefficient (a) r=−0.474, *P*=.0001, (b) r=−0.427, *P*=.0006).

PIOLs, which supports previous reports on the relationship between axial length and visual function. Considering those previous reports, the decrease in the AULCSF with axial length in our data might result from dysfunction at a postreceptoral level in eyes with a long axial length.

Regarding age, our study showed a significant negative correlation between age and the postoperative AULCSF (see Fig 3), and the postoperative AULCSFs were low, especially in three eyes of patients in the sixth decade of life (see Fig 3).

Some studies have reported the relationship between age and visual function in normal eyes.[27-31] Generally, the degradation in contrast sensitivity with age is reported to be primarily caused by a change in optical function with age[27-29] and a decline in the neurosensory elements of vision with age.[30,31] Marcos[27] reported that higher order aberrations increase with age mainly because of changes in the spherical aberration of the crystalline lens. Amano et al[28] measured the ocular and corneal higher order aberrations in 75 normal eyes and reported that ocular coma increases with age mainly because of increases in corneal coma, and the ocular spherical aberration increases with age mainly because of the increase in the spherical aberrations in the internal optics.

In the current results, postoperative S3 and S4 showed multicollinearity with age and were significantly positively correlated with age (see Fig 4). Although these parameters were not entered into the regression model because of the multicollinearity, degradation of retinal images due to increased higher order aberrations with age was assumed to be a reason for loss of postoperative AULCSF in older patients.

Regarding the effect of aging on the neurosensory elements of vision, previous reports have suggested that the neurosensory function degrades with aging.[30,31] Elliott et al[30] compared contrast sensitivity thresholds in young patients with those in older patients and reported a significant reduction in contrast sensitivity in the older group predominantly due to the neural loss within the visual pathways with increasing age rather

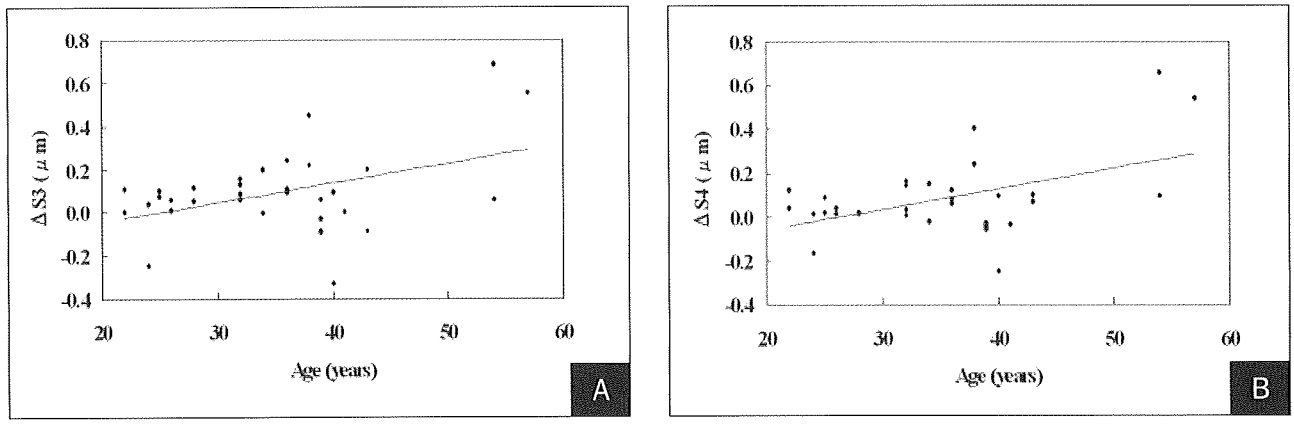

Figure 5. There is a significant correlation between age and **A)** ΔS3 and **B)** ΔS4 (Pearson's correlation coefficient (a) r=0.420, *P*=.018, (b) r=0.486, *P*=.0036).

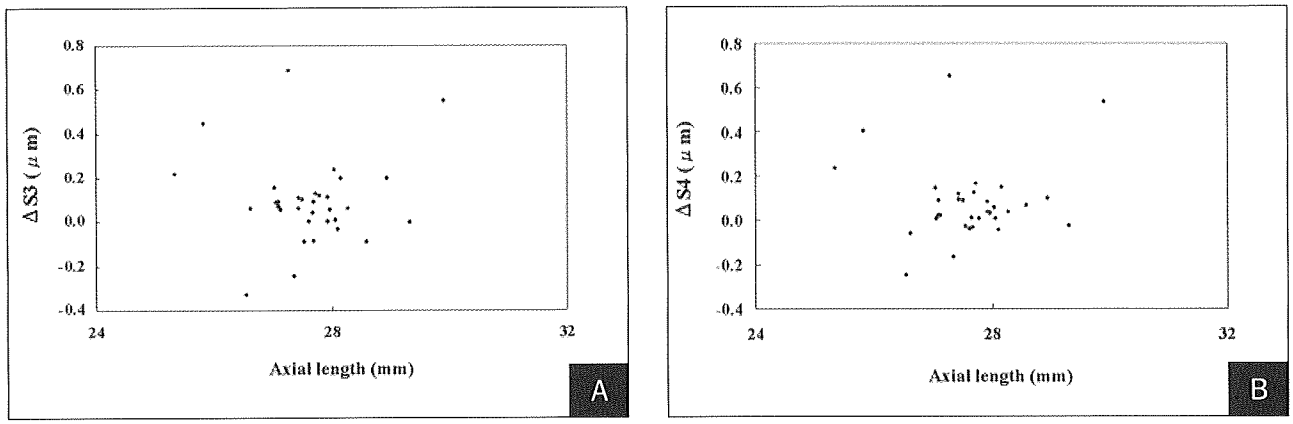

Figure 6. There is no significant correlation between the axial length and **A)** ΔS3 and **B)** ΔS4 (Pearson's correlation coefficient (a) r=−0.188, *P*=.299, (b) r=−0.132, *P*=.468).

than optical changes due to aging. Previous reports suggested that the decreased AULCSF with age in our data might be affected not only by the optical change due to aging but also by the change in neurosensory function with age. Whatever the reason, our data indicated that the postoperative visual function in eyes with Artisan PIOLs is expected to degrade with age.

Some reports on optical and visual function in eyes with PIOLs have been published.[32,33] Lombardo et al[32] studied the pre- and postoperative photopic and mesopic contrast sensitivities in 49 eyes of 30 patients with myopia and myopia with astigmatism who underwent implantation of Artisan PIOLs. The authors reported that compared with preoperative measurements, the postoperative contrast sensitivity increased under photopic conditions and decreased slightly under mesopic conditions.[32] Malecaze et al[33] compared the refractive performance and safety of LASIK with that of Artisan PIOL in 25 patients with myopia ranging from −8.00 to −12.00 D, and reported no significant differences in contrast sensitivity between the two methods at all four spatial frequencies (3, 6, 12, and 18 cpd) at 1-year follow-up, although the contrast sensitivity values were slightly modified in the LASIK-treated eyes and improved in the Artisan-treated eyes.

The current results showed no significant difference in the AULCSF under photopic conditions, which supports the previous reports and suggests that the PIOL, in contrast to LASIK, corrects high myopia without degrading postoperative visual function.

In eyes with an Artisan PIOL, as described previously, postoperative S3 and S4 were excluded from the multiple regression analyses because of multicollinearity with age. However, postoperative higher order aberrations are an important factor affecting visual function in normal and postoperative eyes after refractive surgery. In excimer laser corneal refractive surgeries, postoperative higher order aberrations increase with the amount of the refractive correction,[9,34-36] and postoperative visual function decreases with increases in higher order aberrations.[9,10,37,38] Degradation of visual function is a major problem associated with excimer

laser corneal surgery, although the visual function improved when wavefront-guided methods were introduced.[39]

Only a few reports have been published on postoperative higher order aberrations in eyes with PIOLs. Brunette et al[39] measured the wavefront aberrations in four eyes and analyzed the higher order aberrations for each combination of order (third to seventh) and pupil size (3, 4, and 5 mm). The investigators reported that the mean postoperative RMS values were lower than the mean preoperative RMS values.[39] Buhren et al[40] reported that higher order aberrations increased slightly after implantation of the Artisan PIOL and that induction of Z3,−3 and Z4,0 especially contribute to increased higher order aberrations. The authors also reported that trefoil (Z3,−3) was induced as a result of the incision, whereas the increase of spherical aberration is due to the implant.[40] To our knowledge, the report by Tehrani and Dick[41] includes the most cases on higher order aberrations after PIOL implantation; over 12-month follow-up, the third- and fourth-order higher order aberrations did not increase after foldable iris-claw PIOL implantation in 41 myopic eyes.

Our study, which comprised 60 eyes implanted with Artisan PIOLs, included the most cases among the previous studies. In our results, the higher order aberrations, both S3 and S4, increased significantly after implantation of Artisan PIOLs. Factors that may affect the postoperative third- and fourth-order aberrations are patient age, which is related to the preoperative higher order aberrations and to accommodation; surgically induced aberrations such as coma and astigmatism produced by corneoscleral incision; PIOL decentration; or spherical aberration in a PIOL itself. In our results, patient age and the increases in S3 and S4 (ΔS3, ΔS4) had significant positive correlations (see Fig 5). However, no significant correlations existed between the amount of refractive correction (preoperative spherical equivalent) and ΔS3 or ΔS4 (see Fig 6). The loss of accommodation with aging might be attributed partially to the fact that ΔS3 and ΔS4 were positively correlated with age because the aberrations were measured without cycloplegia in the current study. The effect of accommodation on the higher order aberrations in eyes with PIOLs should be investigated further by measuring aberrations under cycloplegia.

In conclusion, the postoperative visual function in eyes with Artisan PIOLs is affected primarily by patient age and axial length. In general, PIOL decentration and corneoscleral incision induce higher order aberrations that degrade postoperative visual function. However, in this study, surgically induced aberrations showed multicollinearity with age and did not independently affect postoperative visual function. The results in this study suggested that implantation of Artisan PIOL does not affect or degrade the postoperative visual function, but younger patients especially younger than 50 years were more likely to attain better postoperative visual function. Long-term observation is needed to evaluate the effect of aging on visual function after implantation of Artisan PIOL in young patients. The result also suggests that aspherical PIOL may improve postoperative visual function by reducing postoperative spherical aberration in older patients.

REFERENCES

1. O'Doherty M, O'Keeffe M, Kelleher C. Five year follow up of laser in situ keratomileusis for all levels of myopia. *Br J Ophthalmol.* 2006;90:20-23.
2. Sekundo W, Bonicke K, Mattausch P, Wiegand W. Six-year follow-up of laser in situ keratomileusis for moderate and extreme myopia using a first-generation excimer laser and microkeratome. *J Cataract Refract Surg.* 2003;29:1152-1158.
3. Perez-Santonja JJ, Bellot J, Claramonte P, Ismail MM, Alió JL. Laser in situ keratomileusis to correct high myopia. *J Cataract Refract Surg.* 1997;23:372-385.
4. Duffey RJ, Leaming D. US trends in refractive surgery: 2004 ISRS/AAO Survey. *J Refract Surg.* 2005;21:742-748.
5. Bailey MD, Olson MD, Bullimore MA, Jones L, Maloney RK. The effect of LASIK on best-corrected high-and low-contrast visual acuity. *Optom Vis Sci.* 2004;81:362-368.
6. Oshika T, Klyce SD, Applegate RA, Howland HC, El Danasoury MA. Comparison of corneal wavefront aberrations after photorefractive keratectomy and laser in situ keratomileusis. *Am J Ophthalmol.* 1999;127:1-7.
7. Moreno-Barriuso E, Lloves JM, Marcos S, Navarro R, Llorente L, Barbero S. Ocular aberrations before and after myopic corneal refractive surgery: LASIK-induced changes measured with laser ray tracing. *Invest Ophthalmol Vis Sci.* 2001;42:1396-1403.
8. Marcos S, Barbero S, Llorente L, Merayo-Lloves J. Optical response to LASIK surgery for myopia from total and corneal aberration measurements. *Invest Ophthalmol Vis Sci.* 2001;42:3349-3356.
9. Lee HK, Choe CM, Ma KT, Kim EK. Measurement of contrast sensitivity and glare under mesopic and photopic conditions following wavefront-guided and conventional LASIK surgery. *J Refract Surg.* 2006;22:647-655.
10. Alió JL, Montés-Micó R. Wavefront-guided versus standard LASIK enhancement for residual refractive errors. *Ophthalmology.* 2006;113:191-197.
11. Kim TI, Yang SJ, Tchah H. Bilateral comparison of wavefront-guided versus conventional laser in situ keratomileusis with Bausch and Lomb Zyoptix. *J Refract Surg.* 2004;20:432-438.
12. Sakimoto T, Rosenblatt MI, Azar DT. Laser eye surgery for refractive errors. *Lancet.* 2006;367:1432-1447.
13. Alió JL. Advances in phakic intraocular lenses: indications, efficacy, safety, and new designs. *Curr Opin Ophthalmol.* 2004;15:350-357.
14. Chang DH, Davis EA. Phakic intraocular lenses. *Curr Opin Ophthalmol.* 2006;17:99-104.
15. Sanders DR, Vukich JA. Comparison of implantable contact lens and laser assisted in situ keratomileusis for moderate to high myopia. *Cornea.* 2003;22:324-331.

16. Sanders DR, Doney K, Poco M. United States Food and Drug Administration clinical trial of the Implantable Collamer Lens (ICL) for moderate to high myopia: three-year follow-up. *Ophthalmology.* 2004;111:1683-1692.
17. Bloomenstein MR, Dulaney DD, Barnet RW, Perkins SA. Posterior chamber phakic intraocular lens for moderate myopia and hyperopia. *Optometry.* 2002;73:435-446.
18. Uusitalo RJ, Aine E, Sen NH, Laatikainen L. Implantable contact lens for high myopia. *J Cataract Refract Surg.* 2002;28:29-36.
19. Asano-Kato N, Toda I, Hori-Komai Y, Sakai C, Fukumoto T, Arai H, Dogru M, Takano Y, Tsubota K. Experience with the Artisan phakic intraocular lens in Asian eyes. *J Cataract Refract Surg.* 2005;31:910-915.
20. Sarver EJ, Sanders DR, Vukich JA. Image quality in myopic eyes corrected with laser in situ keratomileusis and phakic intraocular lens. *J Refract Surg.* 2003;19:397-404.
21. Nio YK, Jansonius NM, Geraghty E, Norrby S, Koojiman AC. Effect of intraocular lens implantation on visual acuity, contrast sensitivity, and depth of focus. *J Cataract Refract Surg.* 2003;29:2073-2081.
22. Tahzib NG, Bootsma SJ, Eggink FA, Nuijts RM. Functional outcome and patient satisfaction after Artisan phakic intraocular lens implantation for the correction of myopia. *Am J Ophthalmol.* 2006;142:31-39.
23. Applegate RA, Howland HC, Sharp RP, Cottingham AJ, Yee RW. Corneal aberrations and visual performance after radial keratotomy. *J Refract Surg.* 1998;14:397-407.
24. Kora Y, Nishimura E, Kitazato T, Inatomi M, Koide R, Yaguchi S, Ozawa T. Analysis of preoperative factors predictive of visual acuity in axial myopia. *J Cataract Refract Surg.* 1998;24:834-839.
25. Liou SW, Chiu CJ. Myopia and contrast sensitivity function. *Curr Eye Res.* 2001;22:81-84.
26. Jaworski A, Gentle A, Zele AJ, Vingrys AJ, McBrien NA. Altered visual sensitivity in axial high myopia: a local postreceptoral phenomenon? *Invest Ophthalmol Vis Sci.* 2006;47:3695-3702.
27. Marcos S. Are changes in ocular aberrations with age a significant problem for refractive surgery? *J Refract Surg.* 2002;18: S572-S578.
28. Amano S, Amano Y, Yamagami S, Miyai T, Miyata K, Samejima T, Oshika T. Age-related changes in corneal and ocular higher-order wavefront aberrations. *Am J Ophthalmol.* 2004;137:988-992.
29. Fujikado T, Kuroda T, Ninomiya S, Maeda N, Tano Y, Oshika T, Hirohara Y, Mihashi T. Age-related changes in ocular and corneal aberrations. *Am J Ophthalmol.* 2004;138:143-146.
30. Elliott D, Whitaker D, MacVeigh D. Neural contribution to spatiotemporal contrast sensitivity decline in healthy ageing eyes. *Vision Res.* 1990;30:541-547.
31. Jay JL, Mammo RB, Allan D. Effect of age on visual acuity after cataract extraction. *Br J Ophthalmol.* 1987;71:112-115.
32. Lombardo AJ, Hardten DR, McCulloch AG, Demarchi JL, Davis EA, Lindstrom RL. Changes in contrast sensitivity after Artisan lens implantation for high myopia. *Ophthalmology.* 2005;112:278-285.
33. Malecaze FJ, Hulin H, Bierer P, Fournié P, Grandjean H, Thalamus C, Guell JL. A randomized paired eye comparison of two techniques for treating moderately high myopia: LASIK and artisan phakic lens. *Ophthalmology.* 2002;109:1622-1630.
34. Marcos S. Aberrations and visual performance following standard laser vision correction. *J Refract Surg.* 2001;17:S596-S601.
35. Tumbocon JA, Suresh P, Slomovic A, Rootman DS. The effect of laser in situ keratomileusis on low contrast vision. *J Refract Surg.* 2004;20:S689-S692.
36. Ricci F, Scuderi G, Missiroli F, Regine F, Cerulli A. Low contrast visual acuity in pseudophakic patients implanted with an anterior surface modified prolate intraocular lens. *Acta Ophthalmol Scand.* 2004;82:718-722.
37. Kaiserman I, Hazarbassanov R, Varssano D, Grinbaum A. Contrast sensitivity after wave front-guided LASIK. *Ophthalmology.* 2004;111:454-457.
38. Kremer I, Bahar I, Hirsh A, Levinger S. Clinical outcome of wavefront-guided laser in situ keratomileusis in eyes with moderate to high myopia with thin corneas. *J Cataract Refract Surg.* 2005;31:1366-1371.
39. Brunette I, Bueno JM, Harissi-Dagher M, Parent M, Podtetenev M, Hamam H. Optical quality of the eye with the Artisan phakic lens for the correction of high myopia. *Optom Vis Sci.* 2003;80:167-174.
40. Buhren J, Kasper T, Terzi E, Kohnen T. Higher order aberrations after implantation of an iris claw PIOL (Ophtec Artisan) in the phakic eye [German]. *Ophthalmologe.* 2004;101:1194-1201.
41. Tehrani M, Dick HB. Changes in higher-order aberrations after implantation of a foldable iris-claw lens in myopic phakic eyes. *J Cataract Refract Surg.* 2006;32:250-254.

AUTHOR QUERIES

Is there a unit of measure associated with area under the log contrast sensitivity function? If so, please include it throughout the text as well as in the figure axis labels.

Page 2, right column, second paragraph: Please provide the manufacturer (and its location) of Viscot.

The last sentence of the article seems unsubstantiated, as nothing was mentioned about aspheric PIOLs in the article. Okay to omit?

The result also suggests that aspherical PIOL may improve postoperative visual function by reducing postoperative spherical aberration in older patients.

Higher-Order Aberrations Due to the Posterior Corneal Surface in Patients with Keratoconus

Tomoya Nakagawa,[1] *Naoyuki Maeda,*[1] *Ryo Kosaki,*[1] *Yuichi Hori,*[1] *Tomoyuki Inoue,*[1] *Makoto Saika,*[2] *Toshifumi Mihashi,*[2] *Takashi Fujikado,*[1,3] *and Yasuo Tano*[1]

Purpose. This study was designed to investigate higher-order aberrations (HOAs) due to the posterior corneal surface in keratoconic eyes compared with normal eyes.

Methods. We studied 24 normal and 28 keratoconic eyes. The anterior/posterior corneal heights and pachymetric data were obtained with a rotating Scheimpflug camera. HOAs for 6 mm pupils were calculated from the differences between the height data and the best-fit sphere, using an original program for each corneal surface. The reference axes of the measurements were aligned with the primary line of sight. The HOAs were expanded with normalized Zernike polynomials. For each pair of standard Zernike terms for trefoil, coma, tetrafoil, and secondary astigmatism, one value for the magnitude and axis was calculated by Zernike vector analysis.

Results. The mean total corneal HOAs (root mean square [μm]) from the anterior/posterior surfaces were significantly ($P < 0.001$) higher in keratoconic (4.34/1.09, respectively) than in control eyes (0.46/0.15). The mean magnitude of each Zernike vector terms for trefoil, coma, and spherical aberration from the anterior/posterior surfaces was significantly ($P < 0.001$) higher in keratoconic (0.77/0.19, 3.57/0.87, −0.44/0.17) than control eyes (0.09/0.04, 0.33/0.07, 0.25/−0.07), respectively. The mean axes by vector calculation for coma due to the anterior (63.6°) and posterior surfaces (241.9°) were in opposite directions.

Conclusions. Corneal HOAs on both corneal surfaces in keratoconic eyes were higher than in control eyes. Coma from the posterior surface compensated partly for that from the anterior surface. Residual irregular astigmatism in patients with keratoconus wearing rigid gas permeable contact lenses can be estimated by measuring the HOA from the posterior corneal surface. (*Invest Ophthalmol Vis Sci.* 2009;50:2660–2665) DOI: 10.1167/iovs.08-2754

From the Departments of [1]Ophthalmology and [3]Applied Visual Science, Osaka University Medical School, Osaka, Japan; and the [2]Research Institute, Optics Laboratory, Topcon Corporation, Tokyo, Japan.

Supported in part by Grant 18591919 from the Japanese Ministry of Education, Science, Sports, and Culture, Tokyo, Japan.

Submitted for publication August 20, 2008; revised October 17 and November 6, 2008; accepted March 26, 2009.

Disclosure: **T. Nakagawa**, None; **N. Maeda**, None; **R. Kosaki**, None; **Y. Hori**, None; **T. Inoue**, None; **M. Saika**, Topcon Corporation (E); **T. Mihashi**, Topcon Corporation (E); **T. Fujikado**, None; **Y. Tano**, None

Presented in part at the annual meeting of the Association for Research in Vision and Ophthalmology, Fort Lauderdale, Florida, April 2008.

The publication costs of this article were defrayed in part by page charge payment. This article must therefore be marked "*advertisement*" in accordance with 18 U.S.C. §1734 solely to indicate this fact.

Corresponding author: Naoyuki Maeda, Department of Ophthalmology, Osaka University Medical School, Room E7, 2-2 Yamadaoka, Suita, 565-0871, Japan; nmaeda@ophthal.med.osaka-u.ac.jp.

Keratoconus is a corneal disorder characterized by progressive corneal thinning and protrusion. Asymmetric corneal protrusion induces irregular astigmatism leading to impaired visual function.[1,2] Many previous studies have evaluated the deformity and effect on the optical performance of the keratoconic eyes. The typical topographic finding of keratoconus is abnormal localized steepening.[3–6]

The irregular astigmatic component extracted from the topographic data of the corneal anterior surface was significantly correlated with the best spectacle-corrected visual acuity in keratoconic eyes.[7,8] Higher-order aberrations (HOAs) in keratoconic eyes also have been evaluated previously. Wavefront sensing showed significantly larger HOAs in refraction, especially coma-like aberrations, in keratoconic eyes.[9,10] The corneal HOAs calculated from the corneal anterior surface topographic data and the keratometric refractive index in keratoconus also had similar results.[9,11–16]

Rigid gas permeable (RGP) lenses correct the irregular astigmatism of the anterior corneal surface in keratoconic eyes. However, residual refractive aberrations have been detected that are supposed to result from aberrations of the internal optics, that is, the lens and posterior corneal surface.[17–20]

The anterior and posterior corneal curvatures are affected in keratoconus.[21–23] The corneal aberrations calculated from the anterior surface may not be precise, because the contribution of the posterior surface to the corneal optical performance cannot be ignored.[24,25] Evaluating aberrations caused by the posterior corneal surface by analyzing posterior corneal topographic data obtained with a slit-scanning topographer will help to assess more precisely the deformed corneal optical performance.[26,27]

Zernike polynomial expansion has been one of the most useful methods to represent ocular HOAs. The usefulness of the simplified representation of the HOAs expressed as a Zernike vector term has been reported previously,[17,28,29] and allows an understanding of the relation between the anterior and posterior corneal aberrations.

In the present study, the corneal aberrations caused by the refraction on the anterior and posterior surfaces were evaluated separately. The aberrations were calculated from the anterior and posterior corneal heights and pachymetric data obtained with a rotating Scheimpflug camera and then expanded as Zernike vector terms to easily understand the relation between the anterior and posterior corneal aberrations.

Methods

Twenty-four normal control eyes of 24 normal control subjects and 28 keratoconic eyes of 24 patients were studied. The detailed characteristics of the subjects are shown in Table 1. The normal control eyes had no ocular disorders except for refractive errors. Only one eye of each control subject was used. The eyes with keratoconus were diagnosed by one experienced clinician (NM). The criteria for diagnosing keratoconus were the presence of central thinning of the cornea with a Fleischer ring, Vogt's striae, or both, by slit-lamp examination.[9] Eyes with forme fruste keratoconus were not included. Keratoconic eyes

Investigative Ophthalmology & Visual Science, June 2009, Vol. 50, No. 6

TABLE 1. Subject Data

	Controls	Keratoconus	*P*-value
No. cases/eyes	24/24	24/28	
Sex (male/female)	14/10	19/9	0.673*
Age, y (mean ± SD)	37.8 ± 14.2	35.5 ± 9.5	0.778†

* Chi-square test.
† Mann-Whitney rank sum test.

with corneal scarring and a history of acute hydrops or other disorders that affect topographic examinations were excluded.

The research adhered to the tenets of the Declaration of Helsinki. The Institutional Review Board of Osaka University approved this study. Informed consent was obtained from all participants after the purpose of the study and the procedures were explained.

The participants' eyes were examined using a rotating Scheimpflug camera (Pentacam; Oculus, Inc., Wetzlar, Germany). Twenty-five pictures were taken during one scan to reconstruct a three-dimensional model of the entire corneal configuration. All subjects were examined at least twice to confirm the reproducibility of the obtained data. The examination quality data were accessed with a built-in program, and the results with serious errors were excluded.

The rotating camera system (Pentacam; Oculus, Inc.) corrects distortions in the Scheimpflug images based on the geometry of the Scheimpflug principle and the refraction of the anterior surface to show various color-coded maps of anterior segment configurations, including corneal heights and pachymetric data. After this correction, the anterior and posterior corneal heights and pachymetric data of the subjects were exported to spreadsheet software (Excel 2000; Microsoft, Inc., Redmond, WA). These data consisted of numerical values of the anterior and posterior heights, the coordinates of the center of the pupil, and the corneal thickness in increments of 1 μm at the coronal plane and coordinates in increments of 0.1 mm. The HOAs of 6 mm pupils were calculated separately by an original program for the anterior and posterior corneal surfaces. The program expanded the anterior and posterior height data to Zernike polynomials and extracted the components of the ideal wavefront of the best-fit sphere. The aberrations were calculated by multiplying the residual components by the difference in the refractive indices on the anterior and posterior surfaces. The spherical aberrations included by the reference spherical body itself were added to avoid underestimation of the spherical aberrations. The refractive indices of the cornea and aqueous humor in the program were 1.376 and 1.336, respectively. The reference axes of the measurements were aligned with the primary line of sight according to the coordinates of the center of the pupil.

The wavefront aberration was expanded with the normalized Zernike polynomials. For each pair of the standard Zernike terms for trefoil, coma, tetrafoil, and secondary astigmatism, a combined value for the magnitude and axis was calculated by Zernike vector analysis. The detailed formulas to calculate this value for each term were reported previously.[17] In the present study, Zernike vector analysis was used to comprehend the relation between the anterior and posterior corneal aberrations. The axes of the left eyes were transposed about the vertical axis to correct for enantiomorphism of the right eyes.[30]

The averages of the magnitude and axis for each Zernike vector term were calculated by simple averaging of the magnitude and by vector calculation, similar to the well-known method for vector analysis of the cylinder.[17,31] Total HOAs were defined as the root mean square of the magnitudes for the third- and fourth-order aberrations. The magnitude of the spherical aberration was expressed as a positive or negative value and not as an absolute value. The axial range for each Zernike vector term varies according to each rotationally symmetric angle. Based on the ranges of the axis in Zernike vector terms, the angles were doubled in secondary astigmatism, tripled in trefoil, or quadrupled in tetrafoil during the calculation of the average magnitudes and axes in Zernike vector terms.

Data were analyzed using statistical analysis software (Sigma Stat ver. 2.0; SPSS, Inc., Chicago, IL). The χ^2 test was used to compare the sex ratio of the subjects. The Mann-Whitney rank sum test was used to compare the age and the radii of curvature of the anterior and posterior best-fit spheres between the keratoconus group and the control group and to compare the magnitude of the total HOAs, trefoil, coma, tetrafoil, secondary astigmatism, and spherical aberration due to the anterior and posterior corneal surfaces between both groups. $P < 0.05$ was considered significant.

RESULTS

There was no significant difference between the groups in age and sex (Table 1). Figure 1 shows the radii of curvature of the best-fit sphere used to calculate the HOAs for each surface. The means ± SD of the radii of the anterior and posterior best-fit spheres in keratoconic eyes (6.80 ± 0.74 mm and 5.18 ± 0.71 mm, respectively) were significantly shorter compared with control eyes (7.66 ± 0.40 mm and 6.25 ± 0.37 mm) for both corneal surfaces ($P < 0.001$, Mann-Whitney rank sum test).

Figure 2 shows the color-coded maps of the anterior and posterior corneal HOAs from a control eye and a typical keratoconic eye. Although no clinically relevant HOAs were detected in the control eye, an inferior slow pattern—that is, a pattern in which the slow wavefront area was inferior—was detected in the keratoconic eye for the HOAs of the anterior surface. The HOAs from the posterior surface were smaller in the opposite direction—a superior slow pattern—compared with the anterior surface.

Figure 3 shows the simple averages of the magnitudes of the total HOAs and each Zernike vector term for the 6 mm diameter. The means ± SD of the total HOAs due to the anterior and posterior surfaces in keratoconic eyes (4.34 ± 2.71 μm and 1.09 ± 0.66 μm, respectively) were significantly higher ($P < 0.001$, Mann-Whitney rank sum test) than those in control eyes (0.46 ± 0.26 μm and 0.15 ± 0.04 μm) for both corneal surfaces. The HOAs of the anterior surfaces were about three or four times larger than those of the posterior surfaces in both groups. The mean magnitudes of trefoil, coma, tetrafoil, and secondary astigmatism due to the anterior and posterior surfaces were also significantly higher ($P < 0.001$, Mann-Whitney rank sum test) in the keratoconic eyes than in the control eyes. The means ± SD of the spherical aberration due to the anterior

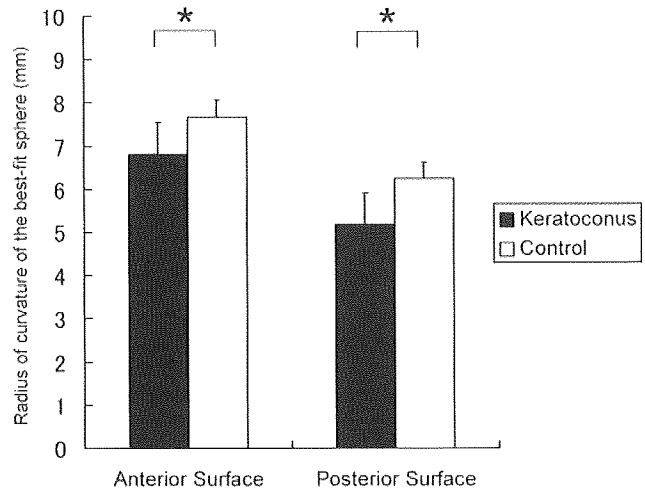

FIGURE 1. The radii of curvature of the best-fit sphere used to calculate HOAs for each surface. The radii of curvature of the best-fit sphere in keratoconic eyes are significantly shorter than those of control eyes for both corneal surfaces. *$P < 0.001$, Mann-Whitney rank sum test.

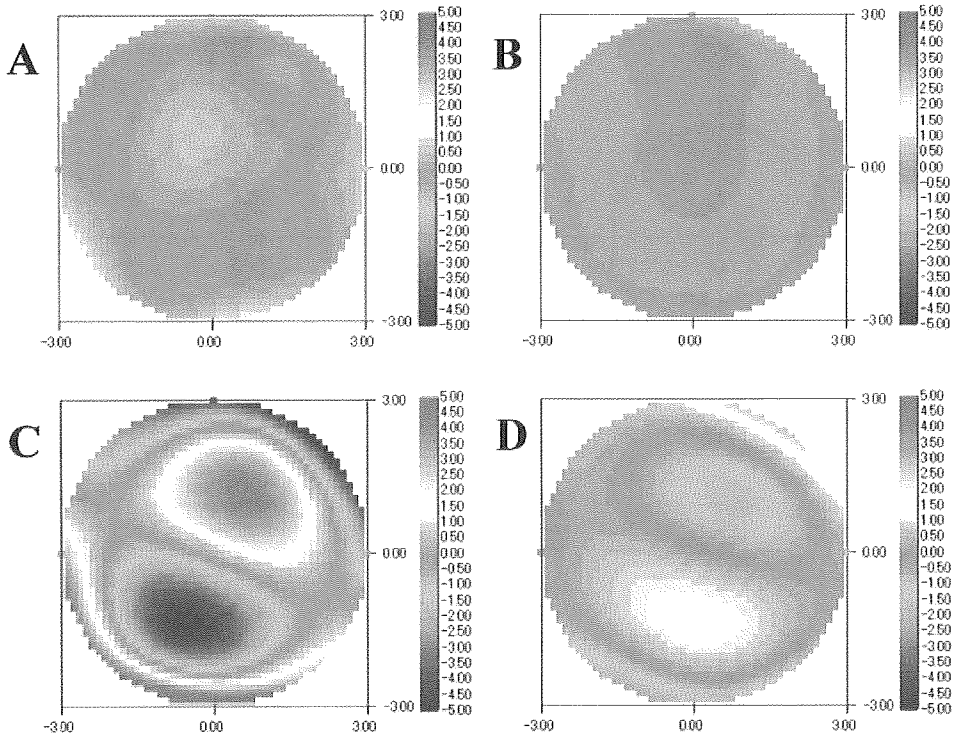

FIGURE 2. Aberration maps of HOAs due to the anterior/posterior corneal surfaces for a normal control eye (**A**, **B**) and a typical keratoconic eye (**C**, **D**). The HOAs from the posterior surface are smaller in the opposite direction than those from the anterior surface.

and posterior surfaces in keratoconic eyes (-0.44 ± 1.37 μm and 0.17 ± 0.40 μm) were significantly different ($P < 0.001$, $P = 0.002$, respectively, Mann-Whitney rank sum test) from those in the control eyes (0.25 ± 0.09 μm and -0.07 ± 0.04 μm) for both corneal surfaces.

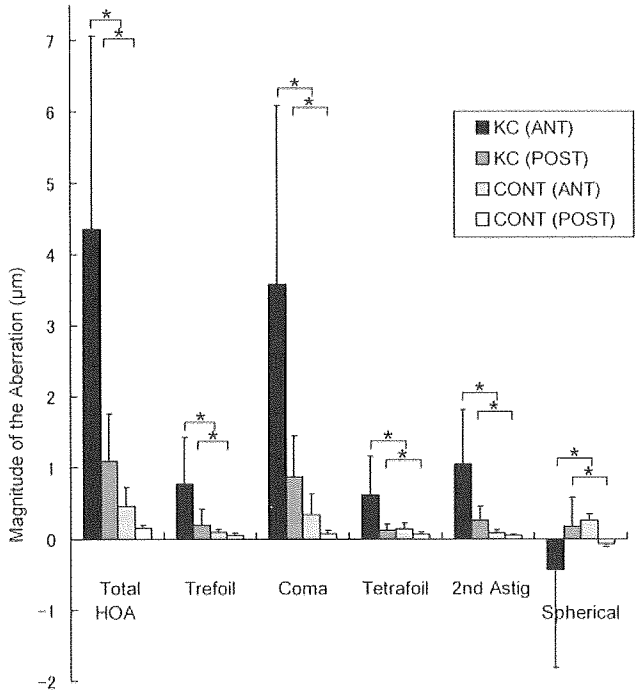

FIGURE 3. The graph shows the simple averages of the magnitudes of the total HOAs (RMS) and each Zernike vector term. The mean total HOAs, trefoil, coma, and spherical aberration due to the anterior and posterior surfaces are significantly higher in the keratoconic eyes than in normal control eyes. *$P < 0.001$, Mann-Whitney rank sum test. ANT, anterior surface; POST, posterior surface; KC, keratoconic eyes; CONT, control eyes; 2nd astig, secondary astigmatism.

Figure 4 shows the Zernike vector terms of trefoil, coma, tetrafoil, and secondary astigmatism due to the anterior and posterior surfaces on the polar coordinates. Regarding trefoil, the axes in most keratoconic eyes ranged from 60° to 120° for the anterior surface, but from 0° to 60° for the posterior surface. Regarding coma, the axes in many keratoconic eyes were distributed around 90° and in some from 45° to 90° for the anterior surface, but the axes were point symmetrically distributed from 180° to 270° for the posterior surface. For both trefoil and coma, the axes in the control eyes were evenly scattered for the anterior and posterior surfaces, and the orientations did not have apparent characteristics. For tetrafoil and secondary astigmatism, no apparent characteristics of the polar coordinates were observed.

Table 2 shows the results of vector calculation of the mean magnitude and axis of each Zernike vector terms for the anterior and posterior surfaces. The axes of coma for the anterior surface in keratoconic eyes (63.6°) and in control eyes (246.3°) were in opposite directions. The axes of trefoil, coma, tetrafoil, and secondary astigmatism for the anterior and posterior surfaces were in opposite directions according to each range of axes in the keratoconic eyes.

DISCUSSION

The main characteristic of the ocular and corneal HOAs in keratoconic eyes has been reported to be increased coma, especially vertical coma.[9,32] The present study also confirmed this pattern for the anterior corneal surface. We previously reported that Zernike vector analysis showed prominent vertical coma with an inferior slow pattern in keratoconic eyes,[17] and we also saw this pattern for the anterior corneal aberrations in the present study. The magnitude of the HOAs from the anterior surface cannot be directly compared with those for the entire cornea in the previous studies, because the refractive indices used to calculate the aberrations differed.

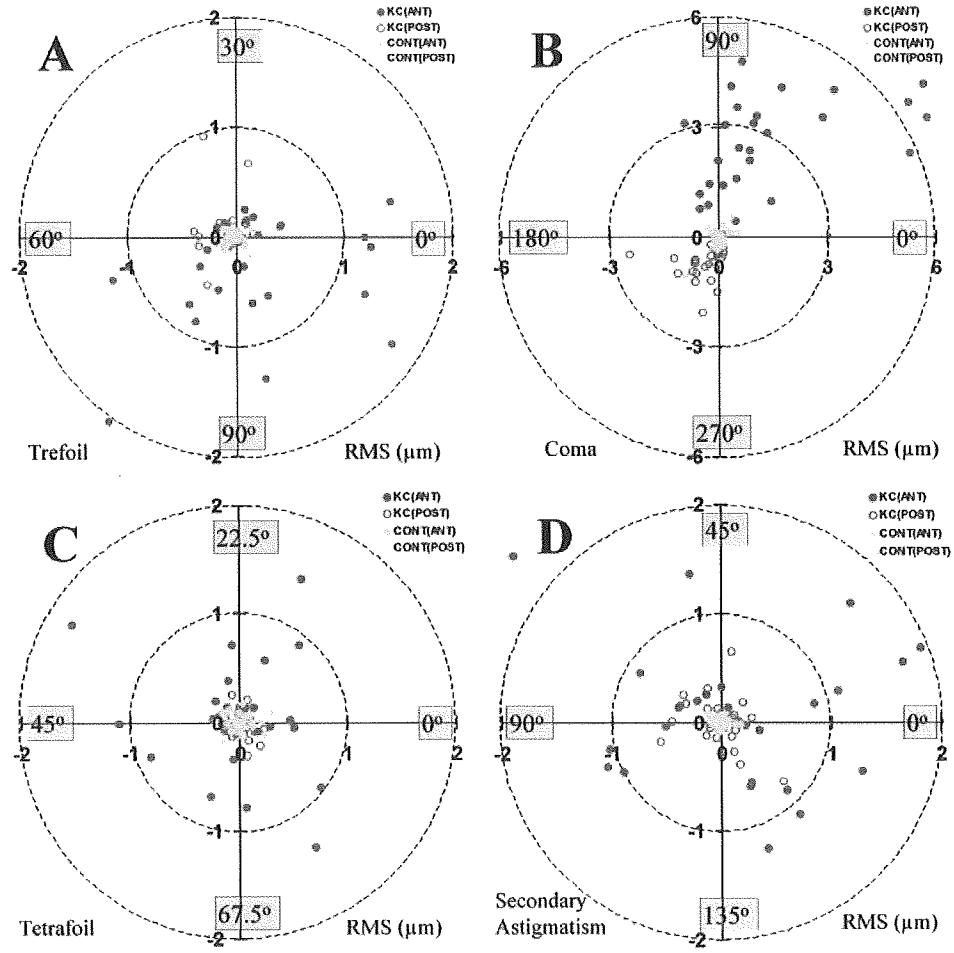

FIGURE 4. Scatterplots of trefoil (**A**), coma (**B**), tetrafoil (**C**), and secondary astigmatism (**D**) in the control and keratoconic eyes. The axes of the coma caused by the anterior and posterior surfaces are generally in opposite directions in the keratoconic eyes.

Although the keratometric index (1.3375) had been used to calculate the anticipated aberration for the entire cornea in our previous studies,[9,17] the refractive indices between the air (1.00) and the cornea (1.376) were used to calculate the corneal anterior aberrations in the present study.

The simple averages of the magnitudes of each Zernike vector term for the anterior surface were three or four times higher than those for the posterior surface. The greater difference in the refractive indices between the air and the cornea for the anterior surface compared with that between the cornea and the aqueous for the posterior surface probably caused these results. The vector calculation of the mean axis of each Zernike vector term for the anterior and posterior surfaces in the keratoconus group showed a mutually reverse pattern for trefoil, coma, tetrafoil, and secondary astigmatism. Increases in the refractive index at the anterior surface yield plus power, and decreases in the refractive index at the posterior surface induce minus power. This difference in the refractive indices and the similar pattern of the corneal configuration between the anterior and posterior surfaces probably caused these results.

The reverse pattern of each Zernike vector term due to the posterior corneal surface may play a role in compensating for the HOAs due to the anterior corneal surface in keratoconic eyes.[33] However, the precise HOAs of the entire cornea are not evaluated from the simple sum of these two, because the incident rays on the posterior surface have a deformed wavefront caused by refraction of the anterior surface. Dubbelman and colleagues reported that after refraction of the anterior surface, the wavefront that approached the posterior surface had the same form as the coma from the posterior surface.[27] Another study, using a virtual ray tracing based on the anterior and posterior surfaces, is needed to calculate more precisely the HOAs of the entire cornea and to evaluate the compensatory effect.[34]

In our previous study, the axes of ocular trefoil and coma were reversed in keratoconic eyes when a RGP lens was

TABLE 2. Vector Calculation of Mean Magnitude and Axis of Each Zernike Vector Term

Group	Trefoil	Coma	Tetrafoil	Secondary Astigmatism
Control				
Anterior surface	0.008@81.2	0.052@246.3	0.008@13.8	0.004@71.6
Posterior surface	0.017@79.7	0.016@293.9	0.010@57.5	0.002@25.9
Keratoconus				
Anterior surface	0.228@102.2	3.260@63.6	0.102@37.6	0.249@169.3
Posterior surface	0.094@46.8	0.779@241.9	0.024@82.9	0.032@92.5

worn.[17] The results of the present study strongly suggested that this reversal was caused mainly by the HOAs of the posterior surface when the RGP lens corrected the irregular astigmatism of the anterior corneal surface. The methods used in this study may enable prediction of the visual quality of a keratoconic eye with a RGP lens even before the lens is worn.

In the present study, we used the rotating camera system (Pentacam; Oculus, Inc.) to obtain a three-dimensional model of the shape of the entire cornea, because the central cornea, which can strongly affect the optical performance, was closely measured by the rotational imaging process. Placido ring-based videokeratography generally has good reproducibility because of rapid measurement, but it cannot measure the geometry of the corneal vertex or the posterior corneal surface. There is the potential for an artifact resulting from erroneously digitized narrowly spaced rings at steepening points in highly irregular corneas. Because there is little chance of this sort of artifact with the slit-scanning topographer, the corneal aberrations in keratoconic eyes with severe corneal protrusion may be evaluated more precisely with the slit-scanning topographer than by Placido ring-based videokeratography. However, movements of an eye being measured during scanning (1.0 seconds/25 scans) might affect the reliability of the obtained data. The rotating camera system can show corneal thickness and corneal curvature parameters, which also are calculated from the corneal height data. Previous studies have shown that the rotating camera (Pentacam; Oculus, Inc.) system provides measurements of central corneal thickness with good reproducibility and repeatability in not only normal eyes but also keratoconic eyes.[35,36] Other studies have reported that posterior and anterior corneal curvature parameters with the rotating camera (Pentacam; Oculus, Inc.) system were highly repeatable.[37,38] However, there also have been reports that the variability in the corneal elevation impaired corneal first-surface wavefront aberrations calculated using corneal topography (Pentacam; Oculus, Inc.).[39] Another study is needed to compare the HOAs from the posterior corneal surface measured according to a different principle.

The present study had some limitations. The effect of the refraction of the anterior surface on the Scheimpflug image was unavoidable, but it is difficult to prove the validity of the correction for these effects in an in vivo deformed cornea.[40–42] This problem would have to be solved to measure a deformed artificial model eye with a closed anterior chamber and the same refractive indices as a human cornea. We excluded patients with severe corneal opacities because the scattered scanning beam made it difficult to precisely digitize the corneal edges, and eyes with forme fruste keratoconus were not included. Another study is needed to determine whether the differences in the HOAs among normal eyes, eyes with forme fruste keratoconus, and eyes with clinical keratoconus could be shown. Measurement errors due to ocular movements during the examination cannot be prevented completely. High-speed three-dimensional anterior segment optical coherence tomography will solve these problems in the near future.[43,44] Smolek and Klyce and colleagues[45–47] reported that the Zernike polynomial fitting routine up to the tenth order caused loss of fine details with an abnormal corneal surface. Further evaluation of more Zernike terms is needed to improve the accuracy of the fitting of the HOAs.

We believe that evaluation of the aberrations due to the posterior corneal surface and Zernike vector analysis allows increased understanding of their characteristics and can be a useful method to assess the optical quality of keratoconic eyes and other corneal disorders. Because the curvature ratios of postoperative eyes between the anterior and posterior corneal surfaces differ from those in normal eyes,[48,49] evaluation of the corneal posterior aberrations also is needed after keratorefractive surgery or lamellar keratoplasty.

References

1. Krachmer JH, Feder RS, Belin MW. Keratoconus and related noninflammatory corneal thinning disorders. *Surv Ophthalmol.* 1984; 28:293–322.
2. Rabinowitz YS. Keratoconus. *Surv Ophthalmol.* 1998;42:297–319.
3. Maguire LJ, Bourne WM. Corneal topography of early keratoconus. *Am J Ophthalmol.* 1989;108:107–112.
4. Rabinowitz YS, McDonnell PJ. Computer-assisted corneal topography in keratoconus. *Refract Corneal Surg.* 1989;5:400–408.
5. Wilson SE, Lin DT, Klyce SD. Corneal topography of keratoconus. *Cornea.* 1991;10:2–8.
6. Maeda N, Klyce SD, Smolek MK, Thompson HW. Automated keratoconus screening with corneal topography analysis. *Invest Ophthalmol Vis Sci.* 1994;35:2749–2757.
7. Oshika T, Tomidokoro A, Maruo K, Tokunaga T, Miyata N. Quantitative evaluation of irregular astigmatism by Fourier series harmonic analysis of videokeratography data. *Invest Ophthalmol Vis Sci.* 1998;39:705–709.
8. Oshika T, Tanabe T, Tomidokoro A, Amano S. Progression of keratoconus assessed by Fourier analysis of videokeratography data. *Ophthalmology.* 2002;109:339–342.
9. Maeda N, Fujikado T, Kuroda T, et al. Wavefront aberrations measured with Hartmann-Shack sensor in patients with keratoconus. *Ophthalmology.* 2002;109:1996–2003.
10. Pantanelli S, MacRae S, Jeong TM, Yoon G. Characterizing the wave aberration in eyes with keratoconus or penetrating keratoplasty using a high-dynamic range wavefront sensor. *Ophthalmology.* 2007;114:2013–2021.
11. Langenbucher A, Gusek-Schneider GC, Kus MM, Huber D, Seitz B. Keratoconus screening with wave-front parameters based on topography height data. *Klin Monatsbl Augenheilkd.* 1999;214:217–223.
12. Schwiegerling J, Greivenkamp JE, Miller JM. Representation of videokeratoscopic height data with Zernike polynomials. *J Opt Soc Am A Opt Image Sci Vis.* 1995;12:2105–2113.
13. Schwiegerling J, Greivenkamp JE. Using corneal height maps and polynomial decomposition to determine corneal aberrations. *Optom Vis Sci.* 1997;74:906–916.
14. Applegate RA, Hilmantel G, Howland HC, Tu EY, Starck T, Zayac EJ. Corneal first surface optical aberrations and visual performance. *J Refract Surg.* 2000;16:507–514.
15. Alio JL, Shabayek MH. Corneal higher order aberrations: a method to grade keratoconus. *J Refract Surg.* 2006;22:539–545.
16. Buhren J, Kuhne C, Kohnen T. Defining subclinical keratoconus using corneal first-surface higher-order aberrations. *Am J Ophthalmol.* 2007;143:381–389.
17. Kosaki R, Maeda N, Bessho K, et al. Magnitude and orientation of Zernike terms in patients with keratoconus. *Invest Ophthalmol Vis Sci.* 2007;48:3062–3068.
18. Negishi K, Kumanomido T, Utsumi Y, Tsubota K. Effect of higher-order aberrations on visual function in keratoconic eyes with a rigid gas permeable contact lens. *Am J Ophthalmol.* 2007;144: 924–929.
19. Choi J, Wee WR, Lee JH, Kim MK. Changes of ocular higher order aberration in on- and off-eye of rigid gas permeable contact lenses. *Optom Vis Sci.* 2007;84:42–51.
20. Barbero S, Marcos S, Merayo-Lloves J. Corneal and total optical aberrations in a unilateral aphakic patient. *J Cataract Refract Surg.* 2002;28:1594–1600.
21. Tomidokoro A, Oshika T, Amano S, Higaki S, Maeda N, Miyata K. Changes in anterior and posterior corneal curvatures in keratoconus. *Ophthalmology.* 2000;107:1328–1332.
22. Tanabe T, Oshika T, Tomidokoro A, et al. Standardized color-coded scales for anterior and posterior elevation maps of scanning slit corneal topography. *Ophthalmology.* 2002;109:1298–1302.
23. Rao SN, Raviv T, Majmudar PA, Epstein RJ. Role of Orbscan II in screening keratoconus suspects before refractive corneal surgery. *Ophthalmology.* 2002;109:1642–1646.

24. Dubbelman M, Weeber HA, van der HeijdeRG, Volker-Dieben HJ. Radius and asphericity of the posterior corneal surface determined by corrected Scheimpflug photography. *Acta Ophthalmol Scand.* 2002;80:379–383.
25. Dubbelman M, Sicam VA, Van der Heijde GL. The shape of the anterior and posterior surface of the aging human cornea. *Vision Res.* 2006;46:993–1001.
26. Oshika T, Tomidokoro A, Tsuji H. Regular and irregular refractive powers of the front and back surfaces of the cornea. *Exp Eye Res.* 1998;67:443–447.
27. Dubbelman M, Sicam VA, van der Heijde RG. The contribution of the posterior surface to the coma aberration of the human cornea. *J Vis.* 2007;7:10.1–8.
28. Campbell CE. A new method for describing the aberrations of the eye using Zernike polynomials. *Optom Vis Sci.* 2003;80:79–83.
29. Oie Y, Maeda N, Kosaki R, et al. Characteristics of ocular higher-order aberrations in patients with pellucid marginal corneal degeneration. *J Cataract Refract Surg.* 2008;34:1928–1934.
30. Smolek MK, Klyce SD, Sarver EJ. Inattention to nonsuperimposable midline symmetry causes wavefront analysis error. *Arch Ophthalmol.* 2002;120:439–447.
31. Jaffe NS, Clayman HM. The pathophysiology of corneal astigmatism after cataract extraction. *Trans Am Acad Ophthalmol Otolaryngol.* 1975;79:OP615-OP630.
32. Schwiegerling J, Greivenkamp JE. Keratoconus detection based on videokeratoscopic height data. *Optom Vis Sci.* 1996;73:721–728.
33. Artal P, Guirao A, Berrio E, Williams DR. Compensation of corneal aberrations by the internal optics in the human eye. *J Vis.* 2001; 1:1–8.
34. Barbero S, Marcos S, Merayo-Lloves J, Moreno-Barriuso E. Validation of the estimation of corneal aberrations from videokeratography in keratoconus. *J Refract Surg.* 2002;18:263–270.
35. Amano S, Honda N, Amano Y, et al. Comparison of central corneal thickness measurements by rotating Scheimpflug camera, ultrasonic pachymetry, and scanning-slit corneal topography. *Ophthalmology.* 2006;113:937–941.
36. de Sanctis U, Missolungi A, Mutani B, Richiardi L, Grignolo FM. Reproducibility and repeatability of central corneal thickness measurement in keratoconus using the rotating Scheimpflug camera and ultrasound pachymetry. *Am J Ophthalmol.* 2007;144:712–718.
37. Chen D, Lam AK. Intrasession and intersession repeatability of the Pentacam system on posterior corneal assessment in the normal human eye. *J Cataract Refract Surg.* 2007;33:448–454.
38. Shankar H, Taranath D, Santhirathelagan CT, Pesudovs K. Anterior segment biometry with the Pentacam: comprehensive assessment of repeatability of automated measurements. *J Cataract Refract Surg.* 2008;34:103–113.
39. Shankar H, Taranath D, Santhirathelagan CT, Pesudovs K. Repeatability of corneal first-surface wavefront aberrations measured with Pentacam corneal topography. *J Cataract Refract Surg.* 2008; 34:727–734.
40. Koretz JE, Strenk SA, Strenk LM, Semmlow JL. Scheimpflug and high-resolution magnetic resonance imaging of the anterior segment: a comparative study. *J Opt Soc Am A Opt Image Sci Vis.* 2004;21:346–354.
41. Dubbelman M, van der Heijde RG, Weeber HA. Comment on "Scheimpflug and high-resolution magnetic resonance imaging of the anterior segment: a comparative study." *J Opt Soc Am A Opt Image Sci Vis.* 2005;22:1216–1218.
42. Dubbelman M, Van der Heijde GL, Weeber HA. Change in shape of the aging human crystalline lens with accommodation. *Vision Res.* 2005;45:117–132.
43. Sarunic MV, Asrani S, Izatt JA. Imaging the ocular anterior segment with real-time, full-range Fourier-domain optical coherence tomography. *Arch Ophthalmol.* 2008;126:537–542.
44. Miura M, Mori H, Watanabe Y, et al. Three-dimensional optical coherence tomography of granular corneal dystrophy. *Cornea.* 2007;26:373–374.
45. Smolek MK, Klyce SD. Zernike polynomial fitting fails to represent all visually significant corneal aberrations. *Invest Ophthalmol Vis Sci.* 2003;44:4676–4681.
46. Klyce SD, Karon MD, Smolek MK. Advantages and disadvantages of the Zernike expansion for representing wave aberration of the normal and aberrated eye. *J Refract Surg.* 2004;20:S537–541.
47. Smolek MK, Klyce SD. Goodness-of-prediction of Zernike polynomial fitting to corneal surfaces. *J Cataract Refract Surg.* 2005;31: 2350–2355.
48. Srivannaboon S, Reinstein DZ, Sutton HF, Holland SP. Accuracy of Orbscan total optical power maps in detecting refractive change after myopic laser in situ keratomileusis. *J Cataract Refract Surg.* 1999;25:1596–1599.
49. Sonego-Krone S, Lopez-Moreno G, Beaujon-Balbi OV, Arce CG, Schor P, Campos M. A direct method to measure the power of the central cornea after myopic laser in situ keratomileusis. *Arch Ophthalmol.* 2004;122:159–166.

after graft reperfusion in 7 patients undergoing liver transplantation. Liver Transpl 7: 783–789.

Keller JC & Linn JE (1990): Central retinal vein occlusion in a heart transplant patient: a case report. J Tenn Med Assoc **83**: 347.

Lerner AB, Sundar E, Mahmood F, Sarge T, Hanto DW & Panzica PJ (2005): Four cases of cardiopulmonary thromboembolism during liver transplantation without the use of antifibrinolytic drugs. Anesth Analg **101**: 1608–1612.

McGrath MA, Wechsler F, Hunyor ABL & Penny R (1978): Systemic factors contributory to retinal vein occlusion. Arch Intern Med **138**: 216–220.

Correspondence:
Young Hee Yoon
Department of Ophthalmology
Asan Medical Centre
388-1 Pungnab-dong
Songpa-gu
Seoul 138-736
Korea
Tel: + 82 2 3010 3675
Fax: + 82 2 470 6440
Email: yhyoon@amc.seoul.kr

The quantitative detection of blurring of vision after eyedrop instillation using a functional visual acuity system

Misaki Ishioka[1,2], Naoko Kato[2,3], Yoji Takano[3,4], Jun Shimazaki[2,3] and Kazuo Tsubota[2,3]

[1]Ryogoku Eye Clinic, Tokyo, Japan
[2]Department of Ophthalmology, Tokyo Dental College, Chiba, Japan
[3]Department of Ophthalmology, Keio University School of Medicine, Tokyo, Japan
[4]Department of Ophthalmology, International University of Health and Welfare, Mita Hospital, Tokyo, Japan

doi: 10.1111/j.1755-3768.2008.01230.x

Editor,

The blurring of vision that occurs after instilling eyedrops is usually temporary, but some patients find this symptom irritating. Sodium hyaluronate (SH) eyedrops are a popular medication for dry eyes. Preservative-free 0.1% SH (0.1SH) and 0.3% SH (0.3SH) (Hyalein Mini®; Santen Pharmaceuticals, Osaka, Japan) are available in Japan. The latter contains a higher concentration of sodium hyaluronate and is used to treat severe dry eyes, but patients sometimes complain of vision disturbance, presumably because of its higher kinematic viscosity. A more viscous artificial tear is reported to reduce contrast sensitivity (Ridder et al. 2005), but conventional methods of measuring visual acuity do not detect the minimal deterioration in visual function that patients sometimes experience. We sought to detect such changes using the recently developed functional visual acuity (FVA) device and software (NIDEK, Gamagori, Japan) (Ishida et al. 2005; Kaido et al. 2006).

The FVA system enables us to examine temporal changes in visual acuity. The Landolt optotypes are displayed automatically on the monitor, with set display times, starting with the baseline best-corrected Landolt visual acuity. The patient indicates the direction of the optotypes with a joystick. If the responses are correct, the optotypes stay the same size. If the patient answers correctly twice, smaller optotypes are presented. If the responses are incorrect, larger optotypes are presented automatically.

We excluded patients with positive vital staining (fluorescein or rose Bengal), a Schirmer test without anaesthesia of less than 5 mm, or tear break-up times less than 5 seconds

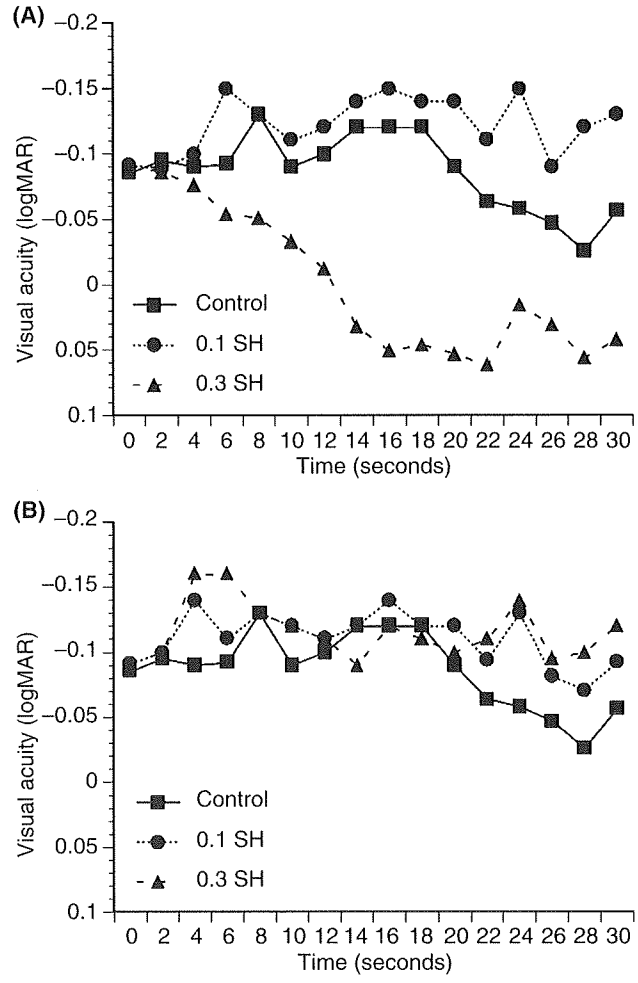

Fig. 1. Mean functional visual acuity of all patients. (A) The functional visual acuity immediately after instilling eyedrops. Over 30 seconds, there was no difference in functional visual acuity between the control group and those with 0.1SH (P = 0.60). With 0.3SH, the functional visual acuity decreased compared to the control group (P = 0.0080). (B) Five minutes after instillation, no significant difference in functional visual acuity was observed among the control, 0.1SH and 0.3SH groups.

Table 1. Change of corneal topography after instilling eyedrops.

	SRI	*P*-value	SAI	*P*-value
Control	0.59 ± 0.46		0.51 ± 0.50	
Immediately after 0.1SH	0.44 ± 0.40	0.076	0.51 ± 0.32	0.70
Immediately after 0.3SH	0.95 ± 0.61	0.010	1.18 ± 1.16	0.0010
5 min after 0.1SH	0.71 ± 0.46	0.44	0.39 ± 0.21	0.52
5 min after 0.3SH	0.70 ± 0.47	0.13	0.48 ± 0.29	0.60

0.1SH, 0.1% sodium hyaluronate; 0.3SH, 0.3% sodium hyaluronate; SRI, surface regularity index; SAI, surface asymmetry index.

and those who were taking medication for ocular diseases and had history of ocular surgery or contact-lens use. Seventeen healthy volunteers (nine male, eight female; 32.8 ± 4.9 years) met these criteria and were enrolled in this study. The lateral eye with more tear secretion was selected for the study. This research was approved by the institutional review board of Ryogoku Eye Clinic and was performed in accordance with the tenets of the Declaration of Helsinki. For the FVA measurement, we selected a 2-second duration for the presentation of optotypes and the patients were allowed to blink freely during the measurements. Topical anaesthesia was not administered. Corneal topography was assessed using the TMS-2N instrument (Tomey Corporation, Nagoya, Japan). Measurements were made immediately after and 5 min after instilling 0.1SH and 0.3SH. Each measurement with different eyedrops was performed on a different day. The eye before using eyedrops served as a control. Two-way analysis of variance (anova) for FVA, Wilcoxon's signed-rank test for the surface asymmetry index (SAI) and surface regularity index (SRI) were used to compare the control and 0.1SH and 0.3SH groups.

During the 30 seconds immediately after instilling 0.3SH, the FVA deteriorated significantly compared to the control, whereas the FVA did not change in the control eye or with 0.1SH (Fig. 1A). Five minutes after instillation, no significant differences were observed among all three groups (Fig. 1B). As shown in Table 1, both the SRI and SAI were increased immediately after instilling 0.3SH, but not with 0.1SH. Five minutes after instillation, no significant differences of SRI and SAI were observed among the three groups. SRI and SAI approach zero for a normally smooth corneal surface and increase directly with irregular astigmatism (Wilson & Klyce 1991). The corneal topography findings implicated irregularity in the tear film in this temporary blurring of vision.

With the FVA system, we were able to detect the transient, short-term blurring of vision caused by viscous eyedrops.

Acknowledgements

The authors thank Ms Chikako Sakai and Ms Yukako Kamiyama for expert technical assistance.

References

Ishida R, Kojima T, Dogru M, Kaido M, Matsumoto Y, Tanaka M, Goto E & Tsubota K (2005): The application of a new continuous functional visual acuity measurement system in dry eye syndromes. Am J Ophthalmol **139**: 253–258.

Kaido M, Dogru M, Yamada M, Sotozono C, Kinoshita S, Shimazaki J & Tsubota K (2006): Functional visual acuity in Stevens–Johnson syndrome. Am J Ophthalmol **142**: 917–922.

Ridder WH III, Lamotte JO, Ngo L & Fermin J (2005): Short-term effects of artificial tears on visual performance in normal subjects. Optom Vis Sci **82**: 370–377.

Wilson SE & Klyce SD (1991): Advances in the analysis of corneal topography. Surv Ophthalmol **35**: 269–277.

Correspondence:
Misaki Ishioka
Ryogoku Eye Clinic
4-33-12 Ryogoku Sumida-ku
Tokyo 130-0026
Japan
Tel: + 81 3 5600 6886
Fax: + 81 3 5669 5888
Email: misaki@misaki-eye.com

Spontaneous calcification of a choroidal melanoma

Béla Csákány and Jeannette Tóth

Department of Ophthalmology, Semmelweis University, Budapest, Hungary

doi: 10.1111/j.1755-3768.2008.01231.x

Editor,

A 28-year-old white male patient was referred with peripheral visual field defect and decreased visual acuity of the right eye. There was no information about systemic disease or metabolic problems in his medical history. In the right eye, we noted thick episcleral sentinel vessels nasally; the anterior segment was quiet and otherwise intact. With funduscopy we observed a highly elevated pigmented mass based nasally at the periphery of the fundus, accompanied by a flat retinal detachment. The clinical diagnosis was choroidal malignant melanoma. The left eye was healthy.

Ultrasound examination showed a smooth, highly reflective surface, medium-to-low homogeneous internal reflectivity with attenuation and numerous fluctuations, and choroidal excavation. There was a circumscribed, highly reflective area with marked acoustic shadowing close to the 'neck' of the mushroom-shaped tumour (Fig. 1A).

A metastatic work-up proved negative. In view of the large size of the tumour (9.4 × 9.3 × 9.2 mm), enucleation was performed.

Histopathological examination confirmed the diagnosis of malignant melanoma, as well as the calcification of the highly reflective part (Fig. 1B). The calcified area was located at the Bruch's membrane and was at the limit between a spindle cell and an epitheloid clone of tumour cells (Fig. 1C). There was no histological evidence of circulation problems (e.g. tumour necrosis) related to the calcified area.

Comment

Ultrasound examination is one of the most informative imaging methods for the diagnosis of intraocular

Clinical and Experimental Ophthalmology 2009; 37: 118–129 doi: 10.1111/j.1442-9071.2009.02005.x

Review

Clinical applications of wavefront aberrometry – a review

Naoyuki Maeda MD
Department of Ophthalmology, Osaka University Medical School, Osaka, Japan

Abstract

One of the most powerful clinical applications of aberrometry is wavefront-guided refractive surgery. This concept led to a paradigm shift in refractive error correction, and the same ideas were applied to design the power and shape of intraocular and contact lenses. Other applications are the diagnosis of irregular astigmatism and the assessments of the optical quality of the eye. Because the higher-order aberrations of the eye are expressed as the total root mean square errors, a set of coefficients for the Zernike terms, Strehl ratio, point spread functions, modulation transfer functions, and other types of metrics can be determined, hence the deterioration in the quality of vision can be easily estimated. Simulations of the retinal images are also useful to understand some of the symptoms in patients with irregular astigmatism. With corneal topographic analyses, the origin of irregular astigmatism from the cornea or internally, or both, can be specified by aberrometry.

Key words: aberration, aberrometry, corneal topography, irregular astigmatism, wavefront.

Introduction

Irregular astigmatism was considered to be a refractive error that could not be corrected with conventional spectacles. Corneal topography was used to diagnose corneal irregular astigmatism, and rigid gas permeable (RGP) contact lenses or corneal transplantations were used to treat these eyes. On the other hand, irregular astigmatism due to the crystalline lens or an intraocular lens (IOL) was not studied in detail because of the difficulties, until recently, in measuring irregular astigmatism caused by the internal optics.

In 1961, the higher-order aberrations (HOAs) of the human eye were first measured by Smirnov using a psychophysical method. He predicted that customized lenses would be made to compensate for the HOAs of individual eyes.[1] A modified technique was developed by Howland,[2] and the wavefront aberrations of the human eye were measured objectively using a Hartmann–Shack sensor in 1994.[3] After the HOAs were successfully corrected using adaptive optics which led to better optical quality of normal eyes,[4] the ability to provide supernormal vision and high-resolution retinal imaging[5] attracted a great deal of attention.

The beginning of the wavefront era began with the development of wavefront-guided refractive surgery,[6] and a paradigm shift occurred in the clinical definition of irregular astigmatism and the concepts of refractive error correction. It was generally assumed that normal eyes did not have irregular astigmatism; however, wavefront analysis showed that there was a small degree of irregular astigmatism even in normal eyes. In addition, the degree of irregular astigmatism was changed by different factors such as blinking, accommodation and ageing. Although there is no obvious influence of mild HOAs on the conventional visual acuity obtained with high-contrast optotypes, the contrast sensitivity and mesopic vision can be worsened.

In this article, the current roles played by aberrometry in the eye clinic will be described by reviewing earlier studies.

Principles

Aberrometry uses wavefront sensing, which is a technique of measuring the complete refractive status, including irregular astigmatism, of an optical

■ **Correspondence:** Dr Naoyuki Maeda, Department of Ophthalmology, Osaka University Medical School, Room J7, Yamadaoka 2-2, Suita 565-0871, Osaka, Japan. Email: nmaeda@ophthal.med.osaka-u.ac.jp

Received 14 August 2008; accepted 11 November 2008.

system. Light is defined differently in geometrical and physical optics. In geometrical optics, the rays from a point source of light radiate out in all directions. Light coming from infinity is considered to be linear bundles of light rays. In physical optics, on the other hand, light is expressed as a wave, and the light waves spread in all directions as a spherical wave. The wavefront is the shape of the light waves that are all in-phase.[7] Light coming from infinity is expressed as proceeding as a plane wavefront.

The differences in the concepts of a lens or an optical system in geometrical and physical optics are shown in Figure 1a. Although the lens is usually defined as the object that refracts the light rays, it can also be considered as the one that transforms the shape of the wavefront. The refractive status of the eye, for example emmetropia, myopia, hyperopia and eyes with HOAs (irregular astigmatism), can be displayed using wavefronts as shown in Figure 1b.

A wavefront aberration is defined as the deviation of the wavefront that originates from the measured optical system from reference wavefront that comes from an ideal optic system. The unit for wavefront aberrations is microns or fractions of wavelengths and is expressed as the root mean square or RMS.

The purpose of wavefront analyses of the eye is to evaluate the optical quality of the eye by measuring the shape of its wavefront as wavefront aberrations. For this, an aberrometer or wavefront sensor is used, and for measuring the corneal wavefront aberrations, a corneal topographer is used.

Aberrometers are usually classified into three types. The first type is the outgoing wavefront aberrometer as in the Hartmann–Shack sensor,[8] and the second type is the ingoing retinal imaging aberrometer as in the cross-cylinder aberrometer,[2] Tscherning aberrometer[9] and the sequential retinal ray tracing method.[10] The third type is the ingoing feedback aberrometer as used in the spatially resolved refractometer[11] and the optical path difference method.[12]

The shape of the wavefront can be analysed by expanding it into sets of Zernike polynomials. The Zernike polynomials are a combination of independent trigonometric functions that are appropriate for describing the wavefront aberrations because of their orthogonality. The first to sixth orders Zernike polynomials are shown graphically in Figure 1c. The zero order has one term that represents a constant. The first order has two terms that represent tilt for the x

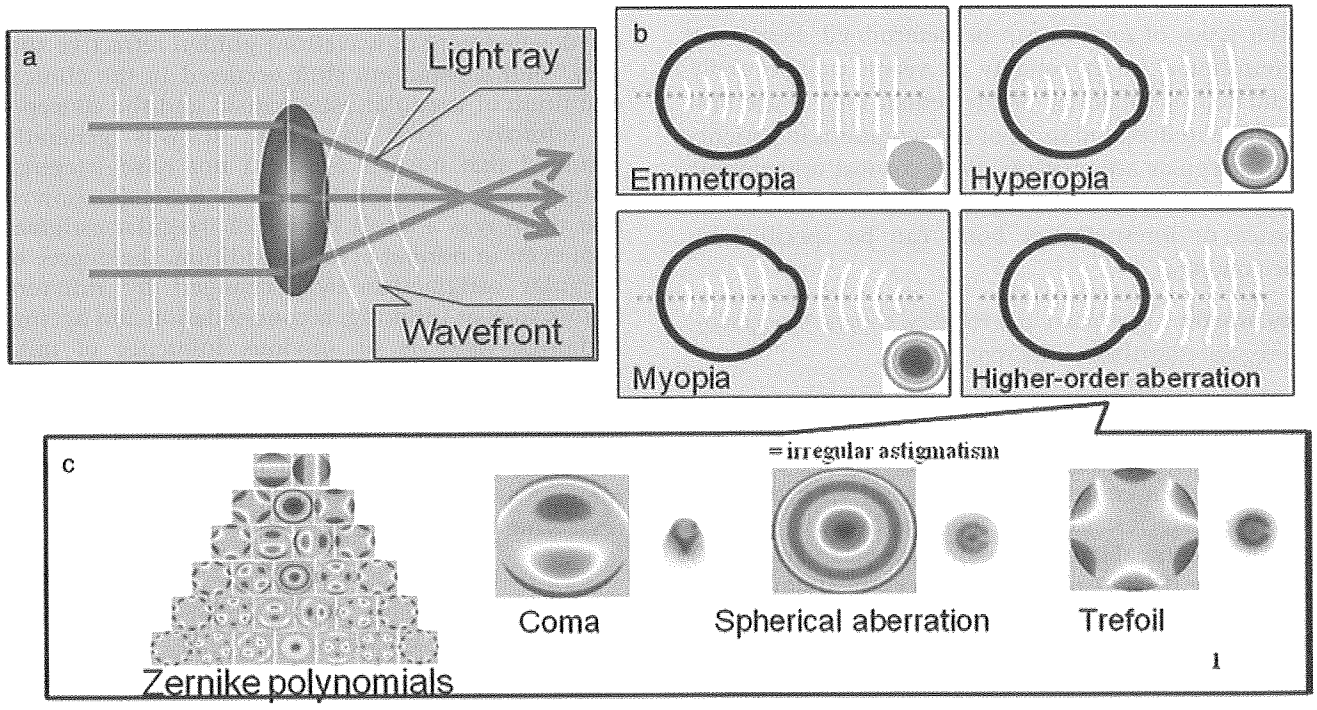

Figure 1. The differences in the concepts of a lens or an optical system in geometrical and physical optics (a). Effect of refractive errors on the wavefront (b). The wavefront of the perfect eye, that is an emmetropic eye without any aberrations, is shown as a perfect plane that is perpendicular to the line of sight. The wavefront in a myopic eye has a bowl-like (concave) shape with the peripheral wavefront more advanced than the central wavefront. The wavefront of the hyperopic eye has a hill-shape (convex shape) with the central wavefront more advanced than the peripheral wavefront. The wavefront of an eye with irregular astigmatism has an irregular and complex shape. The first to sixth orders Zernike polynomials shown graphically (c).

and y axes. The second order includes three terms that represents defocus and regular astigmatism in the two direction. The third order has four terms that represent coma and trefoil, and similarly, the fourth order has five terms that represent tetrafoil, secondary astigmatism and spherical aberration.

The polynomials can be expanded up to any arbitrary order if a sufficient number of measurements are made for the calculations. Spectacles can correct for only the second order aberrations, and not the third- and higher-orders that represent irregular astigmatism. Monochromatic aberrations can be evaluated quantitatively using the Zernike coefficients for each term.

Although the total HOAs can be used to estimate the severity of deterioration of optical quality of the eye as the diagnostic purposes, it will be essential for the surgical treatments to quantify the details of wavefront of the eye using Zernike expansion or Fourier expansion.

Wavefront aberrations caused by the anterior and/or posterior corneal surfaces can be calculated using the height data of the corneal topographers such as videokeratoscopes or slit-scanning corneal topographers.[13]

Wavefront-guided refractive surgery

One of the most important roles of aberrometry in the clinic is to provide aberration data of the eye to the excimer laser for customized ablation. With the development of wavefront analyses, the increase of the HOAs of the eye following conventional photorefractive keratectomy (PRK) has been confirmed.[14,15] Therefore, customized ablation that can correct irregular astigmatism or that can reduce the surgically induced irregular astigmatism might solve some of the problems that are induced by the conventional keratorefractive procedures.

Wavefront-guided refractive surgery is a technique using excimer or other lasers to correct not only the spherical and cylindrical refractive errors but also the HOAs. Seiler *et al.* reported the first application of wavefront-guided laser *in situ* keratomileusis (LASIK) using a Tscherning aberrometer to measure the HOAs.[6] At about the same time, McDonald performed the first wavefront-guided LASIK using data obtained from the Hartmann–Shack wavefront sensor.[16] Wavefront-guided LASIK is safe and effective for primary myopia or myopic astigmatism, and it results in equal or better refractive accuracy and uncorrected visual acuity than conventional LASIK.[17]

Theoretically, correcting irregular astigmatism and eliminating the inherent optical aberrations of normal human eyes should result in obtaining super-normal vision.[18] The theoretical limits of visual performance have been estimated to be between 6/3.6 and 6/1.5 depending on the pupillary diameter.[19] Although the HOAs were only reduced after wavefront-guided LASIK in some cases, they were still less than that after conventional LASIK where the HOAs were generally increased.[17]

There are still so many factors that should be solved to improve the results of wavefront-guided refractive surgery. Those include errors of wavefront registration between measurement and treatment, unpredictable changes of corneal shape due to wound healing and/or biomechanics, fluctuation of HOA, fluctuation of beam profile, and so on.

Ageing

Wavefront analyses have shown that normal eyes not only have small degrees of HOAs, but also that the degree of the HOAs was positively correlated with age. This increase was consistent with the decrease of contrast sensitivity with increasing age.[20] In addition, the total ocular HOAs were lower than the corneal aberrations in most of the younger subjects, whereas the reverse was true in older subjects.[21,22] This indicated that the internal optical surfaces compensated, at least in part,[23] for the aberrations associated with the cornea in most of the younger subjects. However, this compensation was not present in the older subjects.

Another analysis of the effects of ageing on the HOAs showed that the ocular coma increased with age, mainly because of the increase in the corneal coma.[24] On the other hand, the increase in the ocular spherical aberration with age was caused mainly by an increase in the spherical aberration of the internal optics.[24] The ocular aberrations increased abruptly especially after 50 years of age due to the increase of lenticular HOAs. Therefore, customized ablation should be carefully considered especially in presbyopic eyes.[25]

Keratoconus

The characteristic HOA finding in keratoconic eyes is the prominent increase of vertical coma due to a corneal component.[26,27] In addition, the trefoil, tetrafoil and secondary astigmatism are higher in keratoconic eyes. When the directions of each term were analysed by Zernike vector analysis, keratoconic eyes tend to have a reverse coma pattern, that is, a prominent vertical coma with an inferior slow pattern.[28] In addition, the trefoil aberration was the reverse of that of normal eyes.[28] Although the total HOAs were significantly reduced with an RGP lens, the total HOA was still higher than that of normal eyes with an RGP lens.[28,29] Interestingly, the patterns

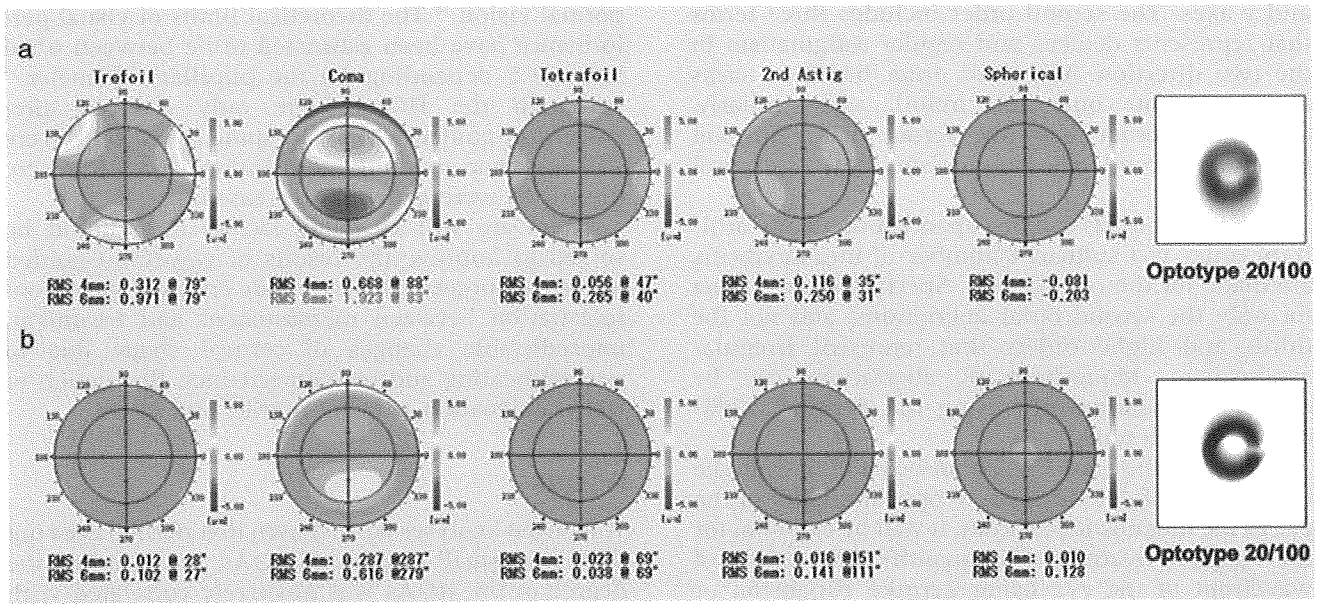

Figure 2. Zernike vector analyses and simulated retinal image of a typical keratoconus case without (a) and with (b) a rigid gas permeable lens (from Kosaki *et al.*[28]). RMS, root mean square.

of the axes of the coma and trefoil were reversed with the RPG lens.[28] The RGP lens corrected the irregular astigmatism; however, smaller comet-like retinal images oriented in the opposite direction remained as a result of the residual vertical coma possibly due to the posterior corneal surface (Fig. 2).

Higher-order aberrations are also used for grading the severity of keratoconus[30] or for detecting keratoconus or keratoconus suspect.[31,32]

Pellucid marginal corneal degeneration

Although pellucid marginal corneal degeneration and keratoconus are categorized as non-inflammatory corneal thinning disorders, the patterns of the HOAs in the two types of eyes differ, possibly owing to differences in the position of the corneal apex.[33] Similar to keratoconic eyes, the mean axes of the coma in eyes with pellucid marginal corneal degeneration are the reverse of that of normal eyes. However, the magnitude of the coma is significantly weaker than that in eyes with keratoconus. The mean axis of the trefoil in this disease or in normal eyes is opposite that in eyes with keratoconus. Also, the sign of the spherical aberration in eyes with pellucid marginal degeneration (plus) is opposite that in eyes with keratoconus (minus).

Periodic examinations of the corneal HOAs in a case of pellucid marginal degeneration showed a gradual and slight increase of the coma-like aberration and stable spherical-like aberration throughout the 11-year observation period.[34]

Post-refractive surgery

Corneal wavefront aberrations have been investigated in patients following radial keratotomy,[35] PRK[36–38] and LASIK.[38,39] The results of several studies have shown that refractive surgeries tended to increase the total HOAs for both day (small pupil) and night vision (large pupil), and the increase was more prominent for night vision than for the day vision.[40] Also, refractive surgeries shifted the aberrations from mainly coma-like aberrations to mainly spherical-like aberrations. The increase in the HOAs was correlated with the amount of refractive correction.[41] These results were directly confirmed by aberrometry as changes in the ocular HOAs (Fig. 3).[42–44]

In terms of wavefront-guided LASIK, a reduction of the HOAs by wavefront-guided PRK or LASIK was found in only some cases, but the residual HOAs were generally lower than that following conventional LASIK.[45–49] Although the HOAs tended to increase,[46,47,50] wavefront-guided ablation also had the advantage over conventional ablation from the standpoint of corneal tissue conservation by some of the instruments.[51]

Wavefront analyses have shown a strong correlation between the visual symptoms and ocular aberrations, for example monocular diplopia in eyes with coma and starburst and glare in eyes with spherical aberration. Thus, aberrometry can also be used to determine the cause of symptomatic LASIK-induced aberrations.[52] To avoid such visual complications, methods that reference the aberration measurements

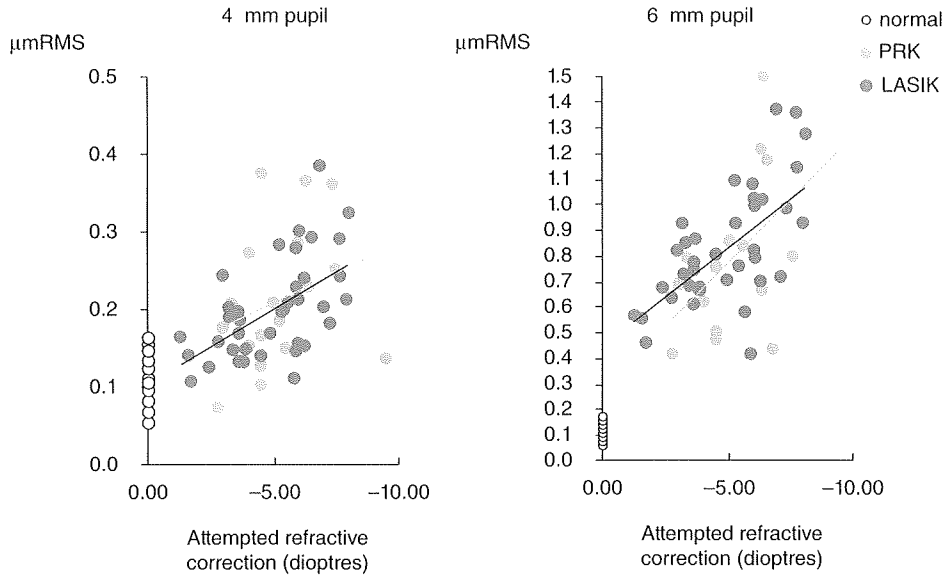

Figure 3. Correlation between the attempted refractive correction and ocular higher-order aberration for a 4 mm and a 6 mm pupillary diameter. The ocular higher-order aberrations increase in proportion to the attempted refractive correction for both photorefractive keratectomy (PRK) and laser *in situ* keratomileusis (LASIK) (from Ninomiya *et al.*[43]).

and treatments[53] to a fixed topological feature of the eye will reduce the potential for inducing aberrations due to shifts in the centre of the pupil.[54]

Tear-film break-up and dry eyes

The first optical surface of the eye is not the surface of the corneal epithelium but the surface of the precorneal tear film. Therefore, it is easy to accept the fact that changes in the tear volume and tear fluid dynamics can induce changes in the HOAs even if the corneal shape is completely ideal. It has been shown that a break-up in the tear-film induces an increase in the ocular HOAs.[55–57] Sequential measurements of the HOAs during a 10-s period after eye opening in normal eyes showed that the post-blink changes in the pattern of the HOAs could be classified into four groups by pattern: stable (Fig. 4a, 25%), small fluctuation (45%), sawtooth (Fig. 4b, 20%) and others (10%).[58] The sequential changes in the total HOAs in subjects with a short tear-film break-up time (TBUT) had a sawtooth pattern with a marked upward curve that increased after blinking.[59] From 5 to 9 s after blinking, the total HOAs were significantly higher than that immediately after blinking, indicating that the optical quality might deteriorate in subjects with a short TBUT by suppressing the blinking. This can arise when staring at a video display terminal even with sufficient tear volume.[59]

On the other hand, increased HOAs were observed in dry eye partially result from superficial punctate keratopathy above the optical zone.[60,61] The low tear volume in severe dry eyes may not cause the sequential increases in the HOAs after blinking,[61] and the time when the minimum RMS aberration occurred was correlated with the TBUTs in mild dry eyes.[62]

In contrast, the sequential post-blink changes in the HOAs had a reverse sawtooth pattern when there was an excessive tear volume in a patient with dry eye who complained of paradoxical visual impairment with epiphora despite an improvement of the dry eye after punctal plug insertion.[63] These results indicated that sequential aberrometry is a useful objective method to evaluate sequential changes of visual performance related to tear-film dynamics. They also indicate that careful measurements and selection of data should be made before wavefront-guided refractive surgery to avoid having used artifactual data because of abnormal tear-film dynamics.[55,64]

Contact lens

Performing aberrometry during contact lens wear is useful for the fitting of contact lenses, and for determining the interaction of the contact lens with the tears, cornea and internal optics of the eye.[65] Even in eyes with identical Snellen visual acuities, the quality of vision can be different in individuals wearing spectacles, soft contact lens and RGP lens. Aberrometry during contact lens and spectacle wear can show the differences in the HOAs.[66] Some studies have shown lower HOAs with RGP lenses than with soft contact lens or spectacles.[65,66] Others have pointed out that vertical coma during RGP wear might be increased or decreased because of preexisting coma[67] or the resting position of contact lenses.

There tended to be an increase in the total HOAs during soft contact lens wear for myopia compared

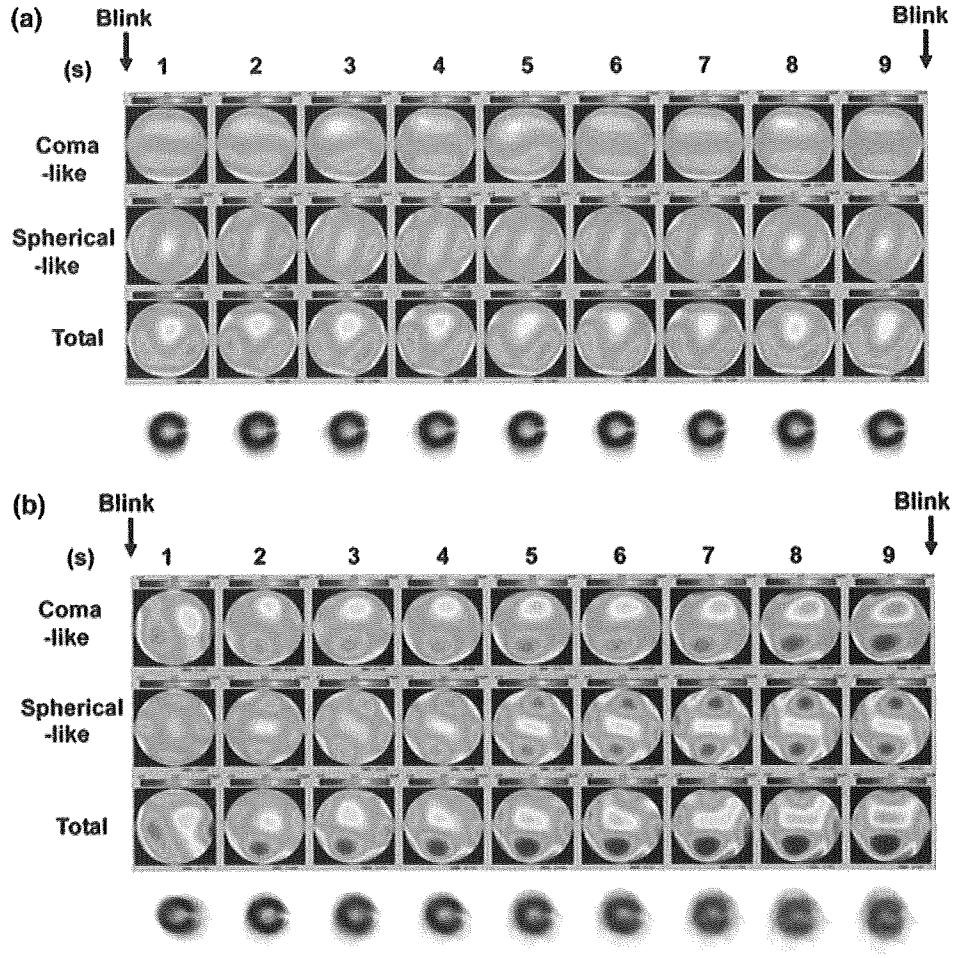

Figure 4. Representative sequential post-blink changes in (a) eyes with a stable pattern and with a (b) sawtooth pattern (from Koh *et al.*[58]).

with those without contact lens wear.[68] Differences in the HOAs can result from the methods used to manufacture the contact lenses,[69] the asphericity of the lenses, the power of the lenses[70] and the flexure of thin RGP lenses.[68] It is well-known that the pre-contact lens tear film is thinner and easier to break-up than the normal pre-corneal tear-film. In symptomatic wearers of disposable soft contact lenses, the use of internal lubricating agents was shown to improve the quality of vision by sequential measurements of the HOAs (Fig. 5).[71]

Because of these factors, for example lens flexure, lens movements, lens decentration and reduced stability of the pre-lens tear film, one needs to remember that there will be larger variability in on-eye than off-eye measurements.[72]

Aberrometry provides a better understanding of the optical effects of contact lenses *ex vivo*[73] or *in situ*, and can be useful for optimizing future designs of contact lenses such as customized soft contact lenses for keratoconic eyes.[74]

Orthokeratology

Corneal HOAs are significantly increased after orthokeratology even in clinically successful cases. The increase in the HOAs was correlated with the magnitude of the myopic correction.[75] Orthokeratology results in reduced low-contrast best-corrected visual acuity because of the increased HOAs.[76,77] A relationship between subclinical decentration and increase of horizontal coma has been suggested to be the cause of the decreased best-corrected visual acuity.[78]

Lenticonus

One of the most interesting applications of wavefront measurements is in the evaluation of lenticular irregular astigmatism qualitatively and quantitatively. This is accomplished by comparing the total HOAs of the eye and those of cornea. Anterior lenticonus due to Alport syndrome had large amount of ocular HOAs with small amount of